DALTON
FULL PAPER

# Synthesis and structural characterisation of ruthenium and osmium carbonyl clusters containing organomercurials

**Fung-Sze Kong and Wing-Tak Wong ***

*Department of Chemistry, The University of Hong Kong, Pokfulam Road, Hong Kong, PR China. E-mail: wtwong@hkucc.hku.hk*

***Received 6th April 1999, Accepted 15th June 1999***

Reaction of the activated cluster $[Os_3(CO)_{10}(NCMe)_2]$ with $[PhHgS(C_5H_4N)]$ afforded two new Os–Hg clusters *cis*-$[Os(CO)_4\{Os_3(CO)_{10}(\mu\text{-}\eta^2\text{-}SC_5H_4N)(\mu\text{-}Hg)\}_2]$ **1** and $[\{Os_3(CO)_{10}(\mu\text{-}\eta^2\text{-}SC_5H_4N)\}_2(\mu_4\text{-}Hg)]$ **2** in 25 and 30% yields, respectively. Cluster **1** consists of two $\{Os_3(CO)_{10}(\mu\text{-}\eta^2\text{-}SC_5H_4N)(\mu\text{-}Hg)\}$ subunits bonded to a central $Os(CO)_4$ moiety in a *cis* configuration. Cluster **2** comprises two skewed Os–Hg metal butterflies sharing a common wingtip Hg atom. Treatment of the same organomercurial with $[Ru_3(CO)_{10}(NCMe)_2]$ produced the cluster compound *cis*-$[Ru(CO)_4\{Ru_3(CO)_9(\mu\text{-}\eta^3\text{-}SC_5H_4N)(\mu\text{-}Hg)\}_2]$ **3** (48%). This has a metal skeleton similar to that of **2** with the $\{S(C_5H_4N)\}$ ligand moiety bonding to the ruthenium atoms in a $\mu\text{-}\eta^3$ fashion. Treatment of $[Os_3(CO)_{10}(NCMe)_2]$ with [PhHg(mbt)] (Hmbt = 2-mercaptobenzothiazole) afforded $[\{Os_3(CO)_{10}(\mu\text{-}\eta^2\text{-}mbt)\}_2(\mu_4\text{-}Hg)]$ **4** (35%) and $[Os_3(CO)_{10}(\mu\text{-}\eta^2\text{-}mbt)(\mu\text{-}\eta^2\text{-}Hg(mbt)]$ **5** (20%). Cluster **4** is very similar to **2**, but the $S(C_5H_4N)$ ligand is replaced by the mbt ligand, while **5** consists of an $Os_3$ triangle having one edge spanned by both $[\mu\text{-}\eta^2\text{-}mbt]$ and $[\mu\text{-}\eta^2\text{-}Hg(mbt)]$ moieties. The reaction of $[Os_5C(CO)_{15}]$ and $[Ru_3(CO)_{12}]$ with another class of organomercurial (diphenylthiocarbazono)phenylmercury reagent [PhHgL′] [L′ = SC(N=NPh)(=NNHPh)] containing a N=N functionality under thermal conditions produced $[\{Os_5C(CO)_{14}(\mu\text{-}\eta^2\text{-}SPh)\}_2(\mu_4\text{-}Hg)]$ **6** (26%) and $[\{Os_5C(CO)_{14}(\mu\text{-}\eta^2\text{-}L')\}_2(\mu_4\text{-}Hg)]$ **7** (34%) and $[Ru_2(CO)_4Ph\{\mu\text{-}\eta^2\text{-}C(O)Ph\}(\mu_2\text{-}S)(\mu\text{-}\eta^2\text{-}L')]$ **8** (15%), $[Ru_2(CO)_4\{C(O)Ph\}\{\mu\text{-}\eta^2\text{-}C(O)Ph\}(\mu_2\text{-}S)(\mu\text{-}\eta^2\text{-}L')]$ **9** (15%) and $[\{Ru(CO)_2Ph\}_2(\mu\text{-}\eta^2\text{-}L')]$ **10** (45%), respectively. In clusters **6** and **7**, two $\{Os_5C(CO)_{14}\}$ subunits linked by a common wingtip mercury atom, are bonded with both $\mu\text{-}\eta^2$-SPh in **6** and $\mu\text{-}\eta^2$-L′ in **7**. However, in the case of complexes **8**, **9** and **10**, only binuclear ruthenium carbonyl complexes formed instead of the expected formation of mixed-metal clusters. Complexes **1**–**10** result from the cleavage of both Hg–C and Hg–S bonds in the parent organomercury species. All these complexes have been fully characterized by both spectroscopic and crystallographic techniques.

## Introduction

Mercury atoms are good 'linkers' in a variety of mixed-metal clusters,[1–5] and this is manifested in their ability to participate in a range of multicentre metal–metal bonds. This may involve the addition of Hg-ligand fragments into a cluster framework or the incorporation of naked Hg atoms or aggregates of Hg atoms into an extended framework. The rich structural chemistry exhibited by osmium–mercury mixed-metal carbonyl clusters has attracted our attention. In preparing these types of mixed-metal cluster compounds, we use the activated clusters $[M_3(CO)_{10}(NCMe)_2]$ (M = Ru or Os) and the carbido cluster $[Os_5C(CO)_{15}]$ in our approach. The use of these complexes as the building blocks in heterometallic clusters as well as in the synthesis of high nuclearity clusters has been well established.[6,7] The generality of a facile Hg–C bond cleavage for aliphatic and aromatic organomercury species upon reaction with triosmium metal clusters has been well demonstrated.[6] However, the reactivity of osmium carbonyl clusters with mercury complexes containing an Hg–S bond has not been thoroughly investigated. In this article we present new results involving this kind of organomercurials with ruthenium and osmium complexes. We describe the preparation of new ruthenium/osmium–mercury carbonyl clusters generated from the reaction of $[M_3(CO)_{10}(NCMe)_2]$ (M = Ru or Os), $[Os_5C(CO)_{15}]$ and $[Ru_3(CO)_{12}]$ with mercury reagents containing Hg–C and Hg–S bonds, namely [PhHgL] [L = $S(C_5H_4N)$ or 2-mercaptobenzothiazole] and [PhHgL′] [L′ = SC(N=NPh)(=NNHPh)] which both contain Hg–C and Hg–S bonds.

## Results and discussion

### Synthesis and crystal structures of *cis*-$[Os(CO)_4\{Os_3(CO)_{10}(\mu\text{-}\eta^2\text{-}SC_5H_4N)(\mu\text{-}Hg)\}_2]$ 1 and $[\{Os_3(CO)_{10}(\mu\text{-}\eta^2\text{-}SC_5H_4N)\}_2(\mu_4\text{-}Hg)]$ 2

Treatment of the activated cluster $[Os_3(CO)_{10}(NCMe)_2]$ with 1 equivalent of $[PhHgS(C_5H_4N)]$ in $CH_2Cl_2$ at room temperature for 2 h afforded two new Os–Hg clusters **1** and **2** in 25 and 30% yields, respectively (Scheme 1). A small amount of metallic mercury has also been isolated. $^1$H NMR spectroscopy (Table 1) showed that both of the pyridyl moieties bonded to the cluster through a sulfur atom and that no orthometallation occurred. To establish the molecular structures of clusters **1** and **2**, single crystal X-ray analyses were carried out on these compounds.

The molecular structure of cluster **1** is depicted in Fig. 1, and selected bond lengths and angles are given in Table 2. The molecule possesses a non-crystallographic two-fold axis. Cluster **1** comprises a central $Os(CO)_4$ fragment bonded to two $\{Os_3(CO)_{10}(\mu\text{-}\eta^2\text{-}SC_5H_4N)(\mu\text{-}Hg)\}$ butterflies in a *trans* configuration. The geometry around Os(1) is octahedrally distorted and the (O)C–Os–C(O) angles range between 96(1) and 101(1)°. The central Hg(1)–Os(7) [2.677(2) Å] and Hg(2)–Os(7) [2.686(2) Å] distances, are significantly shorter than the Hg–Os distances of the $\{Os_3(\mu\text{-}Hg)\}$ units: Hg(1)–Os(1) [2.850(2) Å], Hg(1)–Os(2) [2.797(2) Å], Hg(2)–Os(4) [2.788(2) Å] and Hg(2)–Os(5) [2.849(2) Å]. This is reasonable if one regards the Os–Hg–Os bridges as a three-centre–two-electron bond. The situation is similar to that found in *cis*-$[Os(CO)_4\{Os_3(CO)_{10}(\mu\text{-}\eta^2\text{-}$

**Table 1** Spectroscopic data for compounds **1**–**10**

| Compound | IR, $\nu$(CO)[a]/cm$^{-1}$ | $^1$H NMR,[b] $\delta$ ($J$/Hz) | MS[c] ($m/z$) |
|---|---|---|---|
| **1** | 2099m, 2086w, 2068s, 2051vs, 2018vs, 1989s | 8.81 (2H, d, $J$ = 4.3, aryl H), 7.93 (2H, d, $J$ = 7.7, aryl H), 7.59 (2H, m, aryl H), 7.18 (2H, m, aryl H) | 2627 (2628) |
| **2** | 2095m, 2055s, 2018s, 1989m | 8.43 (2H, m, aryl H), 7.83 (2H, m, aryl H), 7.53 (2H, m, aryl H), 7.11 (2H, m, aryl H) | 2125 (2125) |
| **3** | 2080m, 2069m, 2057m, 2037s, 2023m, 1987s | 8.49 (2H, d, $J$ = 5.3, aryl H), 7.45 (4H, m, aryl H), 7.07 (2H, m, aryl H) | 1948 (1948) |
| **4** | 2111w, 2099m, 2060vs, 2022s, 1993 (sh) | 7.59 (2H, d, $J$ = 8.1, aryl H), 7.37 (2H, d, $J$ = 8.0, aryl H), 7.25 (2H, t, $J$ = 7.7, aryl H), 7.16 (2H, t, $J$ = 7.1, 8.3, aryl H) | 2237 (2237) |
| **5** | 2109s, 2060vs, 2026vs, 2001s | 7.94 (1H, d, $J$ = 8.1, aryl H), 7.67 (1H, d, $J$ = 7.9, aryl H), 7.62 (1H, d, $J$ = 7.9, aryl H), 7.51 (1H, d, $J$ = 8.0, aryl H), 7.37 (1H, t, $J$ = 7.1, 7.7, aryl H), 7.30 (1H, t, $J$ = 7.4, 7.7, aryl H), 7.20 (1H, t, $J$ = 7.3, 7.9, aryl H), 7.10 (1H, t, $J$ = 7.4, 7.6, aryl H) | 1384 (1384) |
| **6** | 2105m, 2072vs, 2059vs, 2032s, 2020s, 2001s, 1962w | 7.55 (4H, d, $J$ = 8.1, aryl H), 7.93 (4H, t, $J$ = 7.7, aryl H), 7.22 (2H, t, $J$ = 7.1, aryl H) | 3125 (3125) |
| **7** | 2099s, 2070vs, 2055w, 2022m, 2010m, 2003m, 1989m, 1943w | 10.76 (2H, s, NH), 7.54 (8H, d, $J$ = 7.8, aryl H), 7.37 (10H, m, aryl H), 7.22 (6H, t, $J$ = 7.2) | 3426 (3426) |
| **8** | 2064m, 2045s, 2001m, 1978m [C=O (KBr) 1563m] | 9.15 (1H, s, NH), 8.10 (2H, d, $J$ = 7.9, aryl H), 7.78 (2H, d, $J$ = 7.1, aryl H), 7.56 (7H, m, aryl H), 7.42 (2H, t, $J$ = 7.2, aryl H), 7.22 (7H, m, aryl H) | 788 (788) |
| **9** | 2064w, 2053vs, 1999s [C=O (KBr) 1561m] | 11.75 (1H, s, NH), 8.26 (2H, m, aryl H), 8.01 (2H, d, $J$ = 8.2, aryl H), 7.86 (2H, d, aryl H), 7.77 (2H, d, $J$ = 7.2, aryl H), 7.55 (12H, m, aryl H) | 811 (811) |
| **10** | 2053s, 2039m, 1976m | 8.90 (2H, s, NH), 7.34 (4H, m, aryl H), 7.20 (6H, t, $J$ = 7.7, aryl H), 7.47 (20H, m, aryl H) | 980 (980) |

[a] In $CH_2Cl_2$. [b] In $CD_2Cl_2$. [c] Simulated values given in parentheses.

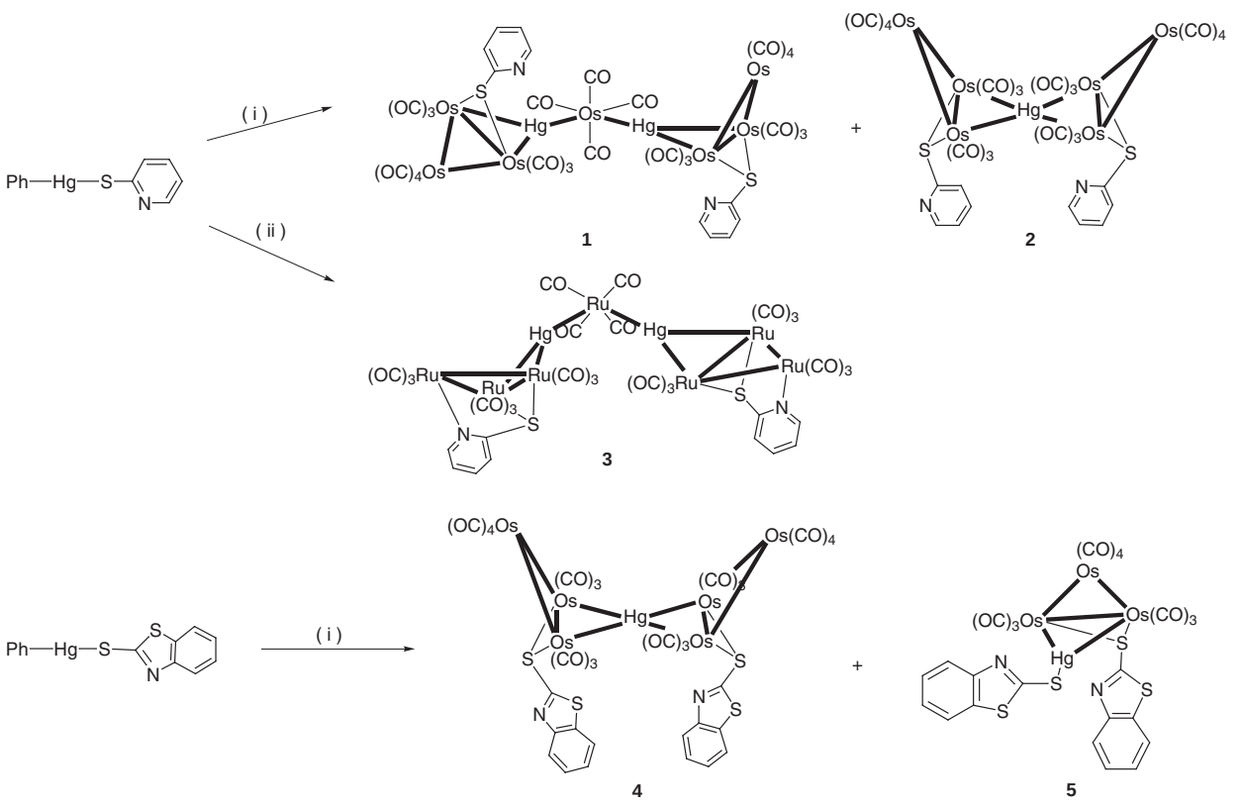


**Scheme 1** (i) $Os_3(CO)_{10}(NCMe)_2$ in $CH_2Cl_2$ at room temp.; (ii) $Ru_3(CO)_{10}(NCMe)_2$ in $CH_2Cl_2$ at room temp.

CH=CHPh)(μ-Hg)}$_2$].[6b] Similar shortenings of M–Hg bonds have been observed in *cis*-[Ru(CO)$_4${Ru$_3$(CO)$_9$(μ$_3$-C≡CMe$_3$)-(μ-Hg)}$_2$],[4] where the difference in the corresponding distances was about 0.16 Å. The intramolecular Hg···Hg distance (3.95 Å) and the Hg(1)–Os(7)–Hg(2) angle [94.73(7)] both indicate very little interaction between the two *cis*-{Os$_3$(CO)$_{10}$(μ-η$^3$-SC$_5$H$_4$N)(μ-Hg)} fragments. Such Hg···Hg interactions were also observed in *cis*-[Os(CO)$_4${Os$_3$(CO)$_{10}$(μ-η$^2$-CH=CHPh)-(μ-Hg)}$_2$][6b] [Hg···Hg 3.700(1) Å and Hg–Os–Hg 87.09(6)°] and *cis*-[Ru(CO)$_4${Ru$_3$(CO)$_9$(μ$_3$-C≡CMe$_3$)(μ-Hg)}$_2$][4] (Hg···Hg 3.55 Å and Hg–Ru–Hg 84°). We can presume that, in general, the shorter the Hg···Hg distance, the smaller the Hg–M–Hg angles and, hence, the larger the interactions between the two Hg subunits. Hg(1) and Hg(2) form a slightly distorted trigonal planar geometry which involves six osmium atoms: Os(1), Os(2), Os(3), Os(4), Os(5) and Os(6). Within each osmium triangle, metal–metal bond distances vary significantly between 2.845(3) and 2.934(3) Å. In particular, the mercury-bridged Os(1)–Os(2) and Os(4)–Os(5) bonding edges are longer than those unsupported Os–Os bonds by a mean distance of 0.06 Å. This may suggest an excess of electrons on the four atoms Os(1), Os(2), Os(4) and Os(5).

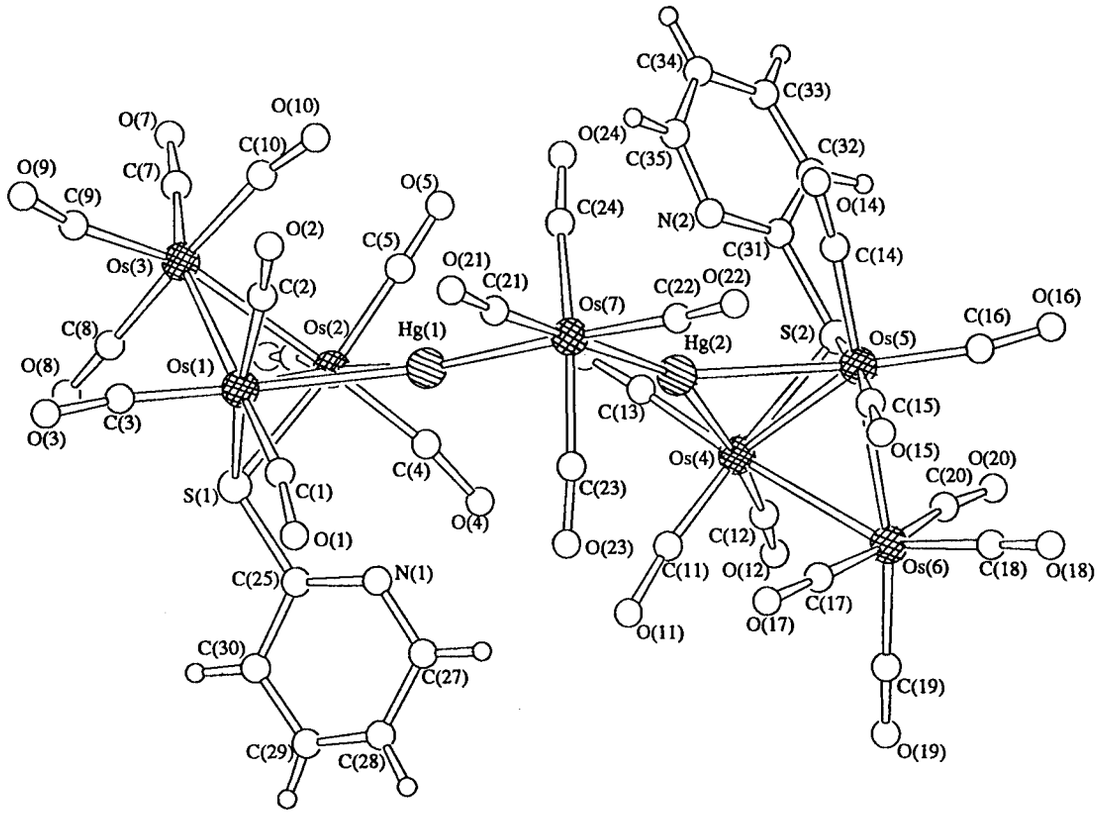


**Fig. 1** A perspective drawing of the molecular structure of **1**.

**Table 2** Selected bond lengths (Å) and angles (°) for complex **1**

| | | | |
|---|---|---|---|
| Hg(1)–Os(1) | 2.850(2) | Hg(1)–Os(2) | 2.797(2) |
| Hg(2)–Os(4) | 2.788(2) | Hg(2)–Os(5) | 2.849(2) |
| Hg(1)–Os(7) | 2.677(2) | Hg(2)–Os(7) | 2.686(2) |
| Os(1)–Os(2) | 2.914(2) | Os(1)–Os(3) | 2.852(3) |
| Os(2)–Os(3) | 2.855(3) | Os(4)–Os(5) | 2.933(3) |
| Os(4)–Os(6) | 2.866(3) | Os(5)–Os(6) | 2.845(3) |
| Os(1)–S(1) | 2.38(1) | Os(2)–S(1) | 2.39(1) |
| Os(4)–S(2) | 2.41(1) | Os(5)–S(2) | 2.40(1) |
| S(1)–C(25) | 1.75(4) | S(2)–C(31) | 1.80(4) |
| Hg(1)···Hg(2) | 3.951(1) | | |
| | | | |
| Hg(1)–Os(7)–Hg(2) | 94.73(7) | Os(1)–Hg(1)–Os(7) | 145.10(8) |
| Os(2)–Hg(1)–Os(7) | 151.46(8) | Os(1)–Hg(1)–Os(2) | 62.12(6) |
| Os(1)–Os(2)–Os(3) | 59.25(6) | Os(2)–Os(1)–Os(3) | 59.34(6) |
| Os(1)–Os(3)–Os(2) | 61.41(6) | Hg(1)–Os(1)–Os(2) | 58.04(6) |
| Hg(1)–Os(2)–Os(1) | 59.83(6) | Os(4)–Hg(2)–Os(7) | 158.72(9) |
| Os(5)–Hg(2)–Os(7) | 137.32(9) | Os(4)–Hg(2)–Os(5) | 62.71(6) |
| Os(4)–Os(5)–Os(6) | 59.45(6) | Os(5)–Os(4)–Os(6) | 58.74(6) |
| Os(4)–Os(6)–Os(5) | 61.81(6) | Hg(2)–Os(4)–Os(5) | 59.67(6) |
| Hg(2)–Os(5)–Os(4) | 57.62(6) | | |

**Table 3** Selected bond lengths (Å) and angles (°) for complex **2**

| | | | |
|---|---|---|---|
| Hg(1)–Os(2) | 2.882(2) | Hg(1)–Os(3) | 2.880(3) |
| Hg(1)–Os(5) | 2.882(2) | Hg(1)–Os(6) | 2.885(3) |
| Os(2)–Os(3) | 2.897(2) | Os(5)–Os(6) | 2.902(2) |
| Os(1)–Os(2) | 2.862(3) | Os(1)–Os(3) | 2.854(3) |
| Os(4)–Os(5) | 2.853(3) | Os(4)–Os(6) | 2.851(3) |
| Os(2)–S(1) | 2.40(1) | Os(3)–S(1) | 2.39(1) |
| Os(5)–S(2) | 2.38(1) | Os(6)–S(2) | 2.39(1) |
| S(1)–C(21) | 1.77(5) | S(2)–C(26) | 1.89(5) |
| | | | |
| Os(2)–Hg(1)–Os(3) | 60.36(6) | Os(5)–Hg(1)–Os(6) | 60.43(6) |
| Hg(1)–Os(2)–Os(3) | 59.78(6) | Hg(1)–Os(3)–Os(2) | 59.86(6) |
| Hg(1)–Os(5)–Os(6) | 59.83(6) | Hg(1)–Os(6)–Os(5) | 59.74(6) |
| Os(1)–Os(2)–Os(3) | 59.42(6) | Os(2)–Os(1)–Os(3) | 60.90(6) |
| Os(1)–Os(3)–Os(2) | 59.68(6) | Os(4)–Os(5)–Os(6) | 59.38(7) |
| Os(5)–Os(4)–Os(6) | 61.16(6) | Os(4)–Os(6)–Os(5) | 59.46(6) |

The solid-state structure of cluster **1** indicates that the two butterflies, and subsequently the two ligand moieties, are arranged in a transoid manner. The central $Os(CO)_4$ linkage is most probably derived from a partial degradation of the parent $Os_3(CO)_{10}$ metal core of the starting material $[Os_3(CO)_{10}(NCMe)_2]$. Similar examples involving an $Os(CO)_4$ linkage have been previously found in *cis*-$[Os(CO)_4\{Os_3(CO)_{10}(\mu\text{-}\eta^2\text{-}CH{=}CHPh)(\mu\text{-}Hg)\}_2]$,[6b] $[Os_3\{\mu\text{-}AuOs(CO)_4(PPh_3)\}(\mu\text{-}Cl)(CO)_{10}]$[8] and $[Hg\{Fe(CO)_4(\mu\text{-}Hg)Fe_3(\mu\text{-}COMe)(CO)_{10}\}_2]$.[9] In all cases, the mechanism of formation of the coordinatively unsaturated $M(CO)_4$ fragments is still unknown, but is presumably derived from the fragmentation of the parent trinuclear metal core.

Dark red crystals of **2** suitable for structural analysis were obtained by standing an *n*-hexane–$CH_2Cl_2$ solution mixture overnight under ambient conditions. An ORTEP drawing of **2** is illustrated in Fig. 2 and some important bond parameters are given in Table 3. The molecular structure reveals a heptametallic Os–Hg metal cluster framework, consisting of two metal butterflies [Os(1), Os(2), Os(3) and Hg(1)] and [Os(4), Os(5), Os(6) and Hg(1)] sharing a common wingtip Hg(1) atom. The two $HgOs_2$ planes are slightly twisted. The skewing is inferred from a non-bonding interaction between the carbonyl ligands on Os(2) and Os(3) and on Os(5) and Os(6). In this context, the geometry around the Hg could be described as pseudo-linear and the dihedral angle between the Hg–Os(2)–Os(3) and Hg–Os(5)–Os(6) planes is 155.04°. Although the solid-state structure of **2** revealed a cisoid configuration, we cannot discard the possibility of other structures such as a transoid arrangement present in solution. It has been shown that the energy barrier to such a rotation is rather low.[10] As in cluster **1**, the mercury-bridged Os(2)–Os(3) [2.897(2) Å] and Os(5)–Os(6) [2.902(2) Å] edges of the two osmium triangles are substantially elongated. The average Os–Os distance in **2** [2.870(1) Å] is shorter than that in **1** [2.977(8) Å] but is almost identical to that in $[Os_3(CO)_{12}]$ [2.877(3) Å].[11] Thus, the overall coordination number around mercury is not a critical factor in determining the bond lengths in this family of complexes, but depends on the overall electronegativity of the group attached to it.

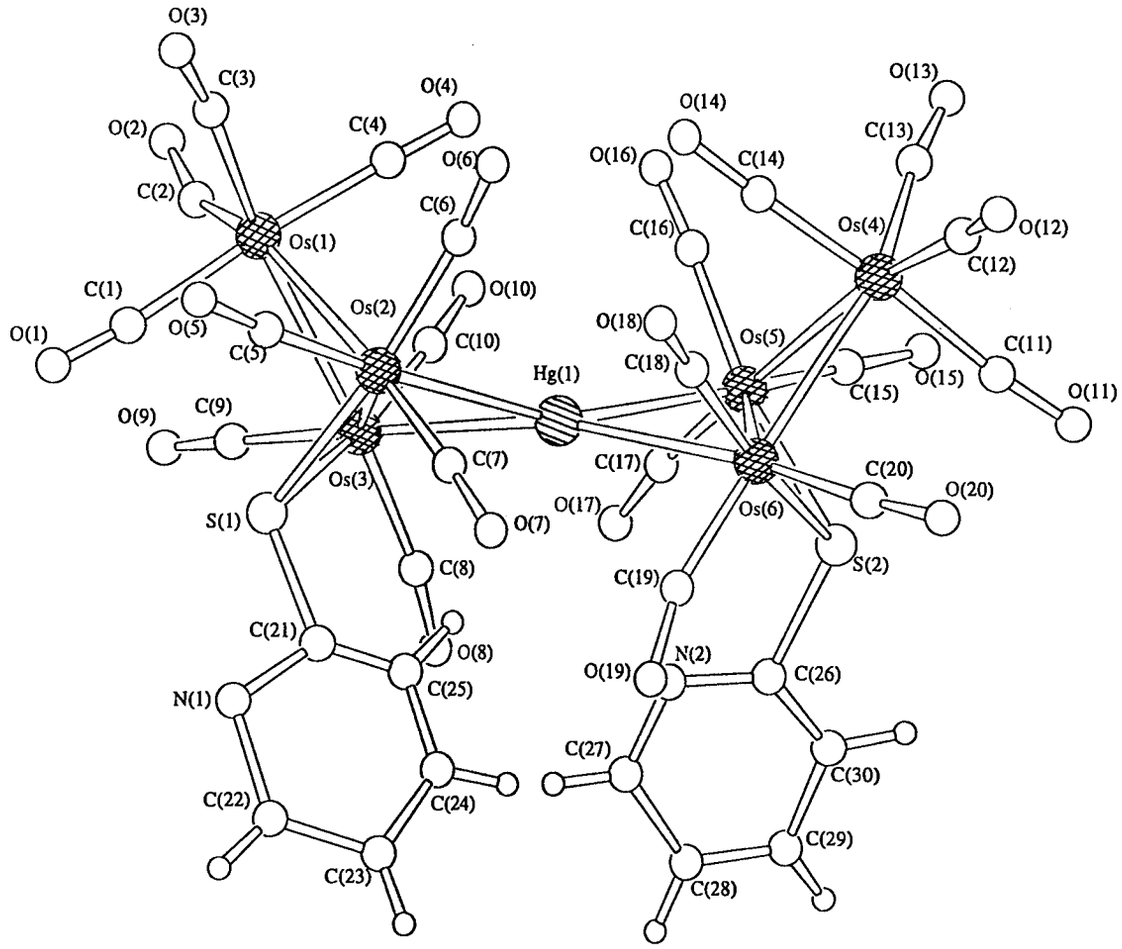


**Fig. 2** A perspective drawing of the molecular structure of **2**.

The organic moieties {S($C_5H_4N$)} in clusters **1** and **2** result in Hg–C and Hg–S bond cleavage of the reactant [PhHgS($C_5H_4N$)]. Their μ-$\eta^2$ bonding mode is reflected from four sets of peaks in the $^1$H NMR spectra. As a whole, the organic moieties bridge along the hinged Os–Os edge as three-electron donors to the cluster valence shell. In essence, the structural properties of the triosmium metal domain in clusters **1** and **2** were similar to those found in [$Ru_3$(μ-H)(μ$_3$-$SC_5H_4N$)$(CO)_9$][12] with the nitrogen atom involved in coordination to the cluster framework. This indicates remarkable rigidity in the metal framework.

### Synthesis and crystal structure of *cis*-[Ru$(CO)_4${$Ru_3(CO)_9$(μ-$\eta^3$-$SC_5H_4N$)(μ-Hg)}$_2$] 3

The organomercury complex [PhHgS($C_5H_4N$)] was allowed to react with the activated ruthenium carbonyl cluster [$Ru_3(CO)_{10}$-$(NCMe)_2$] to yield the cluster *cis*-[Ru$(CO)_4${$Ru_3(CO)_9$($\eta^3$-$SC_5$-$H_4N$)(μ-Hg)}$_2$] **3** as the sole product (Scheme 1). Similar to complex **1**, X-ray analysis of **3** shows that it contains a central 'Ru$(CO)_4$' fragment bound to two [$Ru_3(CO)_9$(μ-$\eta^3$-$SC_5H_4N$)(μ-Hg)] butterflies in a *trans* conformation (Fig. 3). Table 4 lists some selected bond lengths and angles. The {S($C_5H_4N$)} ligand moiety coordinated to the metal core through a nitrogen and sulfur atoms in **3** is coordinated differently from **1** and **2** because the nitrogen atom of the pyridyl ligand is coordinated to the third ruthenium atom [Ru(1)–N(1) 2.21(2) Å, Ru(7)–N(2) 2.20(2) Å]. The {S($C_5H_4N$)} ligand is essentially orthogonal to the ruthenium triangle [dihedral angle 88.05°], which acts as a face capping, five-electron donor. The central Hg(1)–Ru(4) [2.638(3) Å] and Hg(2)–Ru(4) [2.671(3) Å] bond distances are also significantly shorter than the two asymmetric edges bridging the Hg–Ru bonds [average 2.821(2) Å], observed in **1**. The Hg(1)–Ru(4)–Hg(2) bond angle is unusually small [81.62(8)°].

**Table 4** Selected bond lengths (Å) and angles (°) for complex **3**

| | | | |
|---|---|---|---|
| Hg(1)–Ru(4) | 2.638(3) | Hg(2)–Ru(4) | 2.671(3) |
| Hg(1)–Ru(2) | 2.780(3) | Hg(1)–Ru(3) | 2.779(3) |
| Hg(2)–Ru(5) | 2.796(3) | Hg(2)–Ru(6) | 2.806(3) |
| Ru(1)–Ru(2) | 2.793(3) | Ru(1)–Ru(3) | 2.781(4) |
| Ru(2)–Ru(3) | 2.935(3) | Ru(5)–Ru(6) | 2.916(3) |
| Ru(5)–Ru(7) | 2.794(3) | Ru(6)–Ru(7) | 2.790(3) |
| Ru(2)–S(1) | 2.369(8) | Ru(3)–S(1) | 2.378(8) |
| Ru(5)–S(2) | 2.377(8) | Ru(6)–S(2) | 2.362(8) |
| Ru(1)–N(1) | 2.21(2) | Ru(7)–N(2) | 2.20(2) |
| S(1)–C(23) | 1.71(3) | S(2)–C(32) | 1.74(3) |
| Hg(1)···Hg(2) | 3.470(2) | | |
| | | | |
| Hg(1)–Ru(4)–Hg(2) | 81.62(8) | Ru(2)–Hg(1)–Ru(4) | 147.86(9) |
| Hg(1)–Ru(2)–Ru(3) | 58.11(7) | Hg(1)–Ru(3)–Ru(2) | 58.14(7) |
| Hg(2)–Ru(5)–Ru(6) | 58.80(7) | Hg(2)–Ru(6)–Ru(5) | 58.48(7) |
| Ru(3)–Hg(1)–Ru(4) | 146.89(9) | Ru(2)–Hg(1)–Ru(3) | 63.75(7) |
| Ru(1)–Ru(2)–Ru(3) | 58.03(8) | Ru(2)–Ru(1)–Ru(3) | 63.55(9) |
| Ru(1)–Ru(3)–Ru(2) | 58.42(8) | Ru(4)–Hg(2)–Ru(5) | 151.60(8) |
| Ru(4)–Hg(2)–Ru(6) | 145.26(8) | Ru(5)–Hg(2)–Ru(6) | 62.73(7) |
| Ru(5)–Ru(6)–Ru(7) | 58.60(8) | Ru(5)–Ru(7)–Ru(6) | 62.95(8) |
| Ru(6)–Ru(5)–Ru(7) | 58.45(8) | | |

The intramolecular Hg(1)···Hg(2) distance is 3.470(2) Å. The shortening of this non-bonding distance suggests that there may be a significant Hg(1)–Hg(2) interaction, causing an unusually small bond angle of 81.62(8)° between the two mercury atoms.

### Synthesis and crystal structures of [{$Os_3(CO)_{10}$(μ-$\eta^2$-mbt)}$_2$-(μ$_4$-Hg)] 4 and [$Os_3(CO)_{10}$(μ-$\eta^2$-mbt){μ-$\eta^2$-Hg(mbt)}] 5

To test the general Hg–C and Hg–S bond cleavage observed for [PhHgS($C_5H_4N$)], we have investigated the reaction of [$Os_3(CO)_{10}(NCMe)_2$] with another class of organomercury

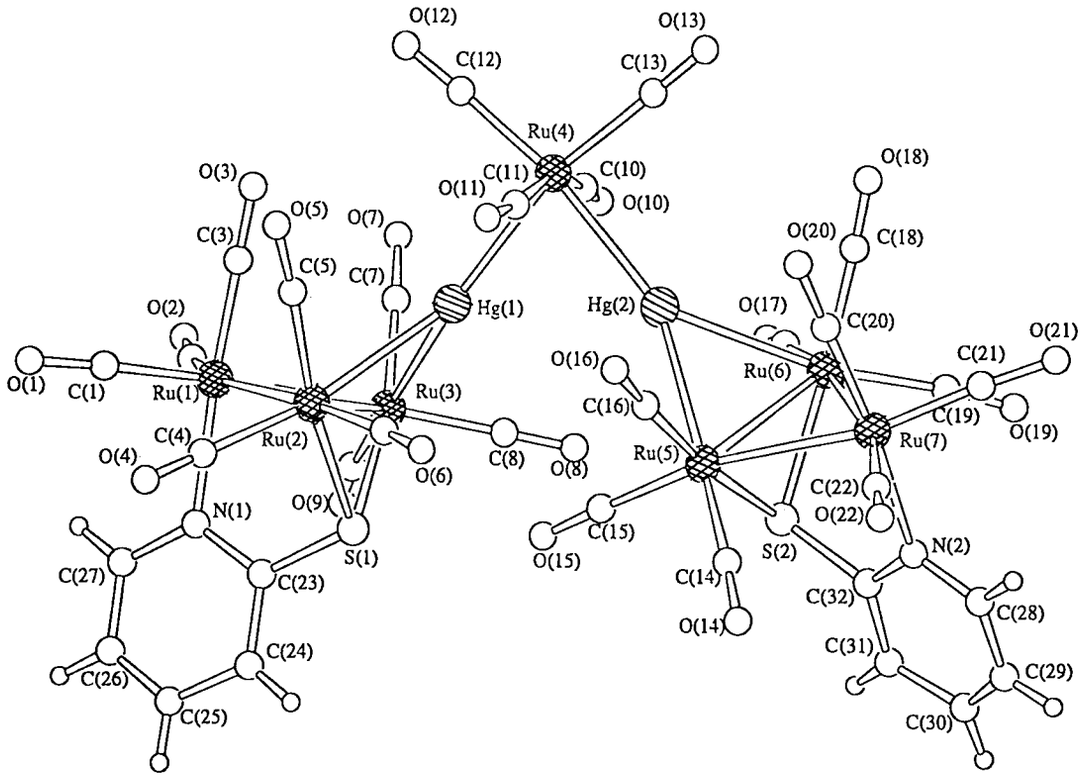


**Fig. 3** A perspective drawing of the molecular structure of **3**.

**Table 5** Selected bond lengths (Å) and angles (°) for complex **4**

| | | | |
|---|---|---|---|
| Hg(1)–Os(1) | 2.861(3) | Hg(1)–Os(2) | 2.903(3) |
| Hg(1)–Os(4) | 2.865(3) | Hg(1)–Os(5) | 2.895(3) |
| Os(1)–Os(2) | 2.897(3) | Os(4)–Os(5) | 2.908(3) |
| Os(1)–Os(3) | 2.871(3) | Os(2)–Os(3) | 2.865(3) |
| Os(4)–Os(6) | 2.866(4) | Os(5)–Os(6) | 2.868(4) |
| Os(1)–S(1) | 2.38(2) | Os(2)–S(1) | 2.38(2) |
| Os(4)–S(3) | 2.41(1) | Os(5)–S(3) | 2.42(1) |
| S(1)–C(41) | 1.74(5) | S(3)–C(48) | 1.73(6) |
| | | | |
| Os(1)–Hg(1)–Os(2) | 60.34(8) | Os(4)–Hg(1)–Os(5) | 60.63(7) |
| Hg(1)–Os(1)–Os(2) | 60.55(8) | Hg(1)–Os(2)–Os(1) | 59.11(8) |
| Hg(1)–Os(4)–Os(5) | 60.19(7) | Hg(1)–Os(5)–Os(4) | 59.18(7) |
| Os(1)–Os(2)–Os(3) | 59.76(1) | Os(2)–Os(1)–Os(3) | 59.58(7) |
| Os(1)–Os(3)–Os(2) | 60.66(7) | Os(4)–Os(5)–Os(6) | 59.48(8) |
| Os(5)–Os(4)–Os(6) | 59.57(8) | Os(4)–Os(6)–Os(5) | 60.94(8) |

compounds [PhHg(mbt)] (Hmbt = 2-mercaptobenzothiazole) to afford [{$Os_3(CO)_{10}(\mu\text{-}\eta^2\text{-mbt})\}_2(\mu_4\text{-Hg})$] **4** and [$Os_3(CO)_{10}(\mu\text{-}\eta^2\text{-mbt})\{\mu\text{-}\eta^2\text{-Hg(mbt)}\}$] **5** in 35 and 20% yields, respectively. IR spectroscopy [$\nu$(CO)] indicates that the metal framework of cluster **4** is quite similar to that of **2** (Table 1). For complex **5** two set of signals, indicative of four aryl protons, appeared in the $^1$H NMR spectrum showing a different environment for two ligand moieties. We believe that Hg–C and Hg–S bond cleavage had occurred. In order to establish the molecular structures of clusters **4** and **5**, X-ray analyses were carried out.

The ORTEP drawings of clusters **4** and **5** are depicted in Figs. 4 and 5, respectively, while selected bond lengths and angles are listed in Tables 5 and 6, respectively. As expected, cluster **4** has the same metal framework as cluster **2**, which consists of two metal butterflies sharing a common wingtip Hg atom. There are two asymmetric units present in the molecule. As a consequence of Hg–C and Hg–S bond cleavage, only the mbt moiety is coordinated to the osmium triangle. In this context, the average dihedral angles of the two butterflies, the twist angle about the central Hg atom, and the average Os–Os bond distance in cluster **4** are 105.23, 39.91° and 2.88 Å, respectively. Consequently, it is reasonable to assume that both clusters adopt a skewed cisoid configuration in their solid-state structures.

**Table 6** Selected bond lengths (Å) and angles (°) for complex **5**

| | | | |
|---|---|---|---|
| Hg(1)–Os(2) | 2.774(1) | Hg(1)–Os(3) | 2.7996(9) |
| Os(2)–Os(3) | 2.925(1) | Os(1)–Os(2) | 2.884(1) |
| Os(1)–Os(3) | 2.872(1) | Hg(1)–S(1) | 2.423(5) |
| Os(2)–S(3) | 2.418(5) | Os(3)–S(3) | 2.421(5) |
| S(1)–C(11) | 1.73(2) | S(3)–C(18) | 1.78(2) |
| | | | |
| Os(2)–Hg(1)–Os(3) | 63.32(3) | Hg(1)–Os(2)–Os(3) | 58.77(3) |
| Hg(1)–Os(3)–Os(2) | 57.91(2) | Os(1)–Os(2)–Os(3) | 59.26(3) |
| Os(2)–Os(1)–Os(3) | 61.09(3) | Os(1)–Os(3)–Os(2) | 59.65(3) |
| Os(2)–S(3)–Os(3) | 74.4(1) | Os(2)–Os(3)–S(3) | 52.8(1) |
| Os(3)–Os(2)–S(3) | 52.9(1) | | |

The metal core of **5** comprises a butterfly framework where the Os(2)–Os(3) edge and the Os(1) and Hg(1) atoms form the hinge and the wingtips of the butterfly. In addition, the Os(2)–Os(3) edge is doubly bridged by an mbt and an Hg(mbt) moiety, as shown in Fig. 5. The Os–Os vector, doubly-bridged by a bridgehead sulfur atom and an Hg atom [Os(2)–Os(3) 2.925(1) Å], is slightly longer than the two unsupported Os–Os bonds [Os(1)–Os(2) 2.884(1) and Os(1)–Os(3) 2.872(1) Å]. This lengthening may be due to the larger size of the sulfur and Hg atoms. Churchill and Lachewycz[13] have shown that a larger bridgehead atom has a larger lengthening effect on the bridged metal–metal bond. The dihedral angle between the metal butterfly is 141.31°. The salient feature of **5** reveals that one of the Hg(mbt) moieties has undergone Hg–S bond cleavage upon coordinating to the cluster framework, while the second Hg(mbt) moiety remains intact on the cluster. Similar coordination modes have been found in [$Ru_3(\mu\text{-HgBr})(\mu_3\text{-ampy})(CO)_9$] [Hampy = 2-amino-6-methylpyridine] in which the ligand ampy and an HgBr moiety bridge across the same Ru–Ru edge.[14]

### Synthesis and crystal structures of [{$Os_5C(CO)_{14}(\mu\text{-}\eta^2\text{-SPh})\}_2(\mu_4\text{-Hg})$] 6 and [{$Os_5C(CO)_{14}(\mu\text{-}\eta^2\text{-SC(N=NPh}_2)\}_2(\mu_4\text{-Hg})$] 7

The reaction of [$Os_5C(CO)_{15}$] with [PhHgSC(N=NPh)(=NNHPh)] in refluxing $CHCl_3$ afforded two new Os–Hg clusters **6** and **7** in 26% and 34% yields, respectively (Scheme 2). The

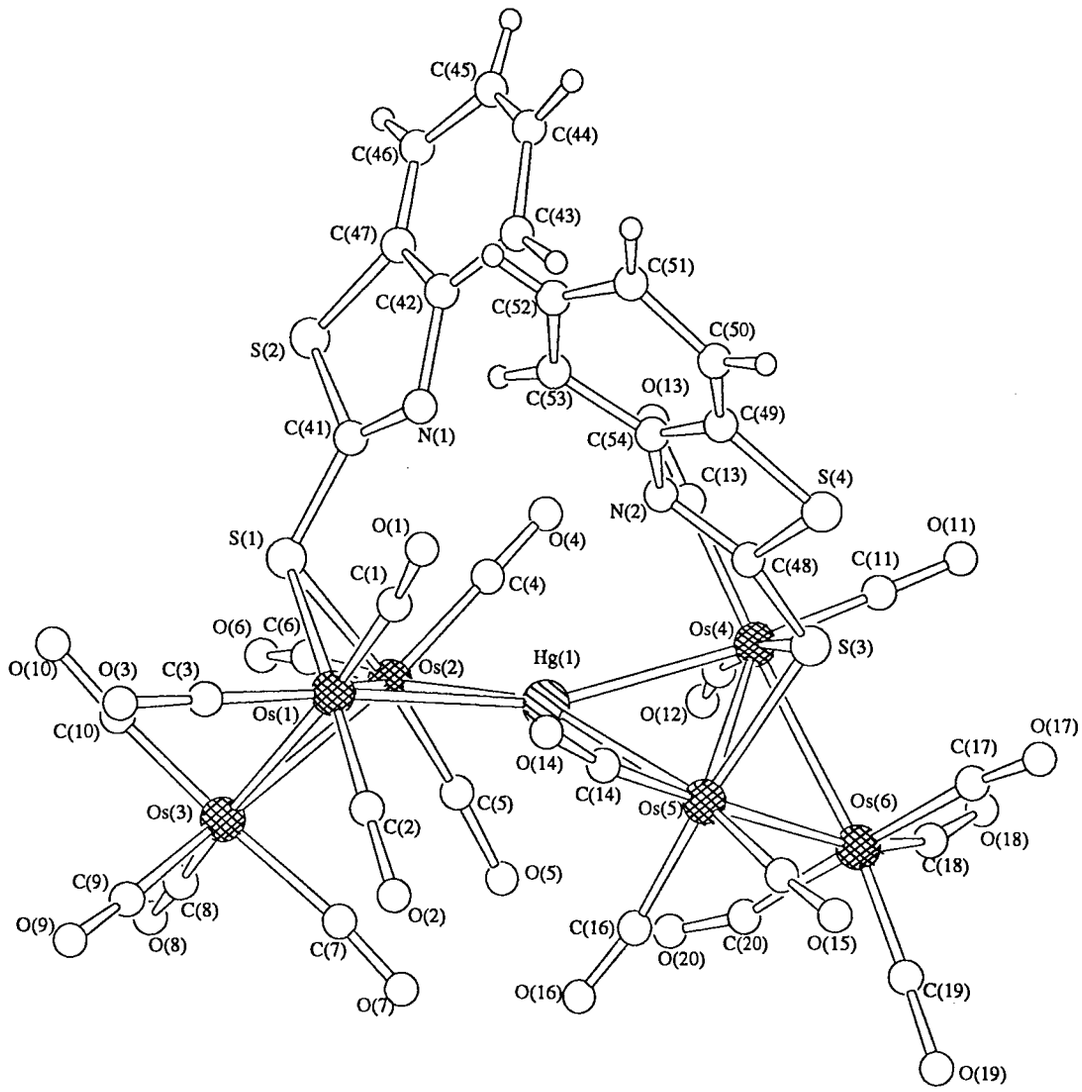


**Fig. 4** A perspective drawing of the molecular structure of **4**.

$^1$H NMR signals due to the organic moieties of both complexes are fully consistent with their structures. The mass spectra exhibit molecular ion envelopes which agree with the formulae of the compounds, with ion peaks corresponding to CO losses also detected. The signals due to protons of the phenyl rings are observed in the range $\delta$ 7.22–7.93 while a broad signal at $\delta$ 10.76 in **7** is assigned to the NH protons of the dithizonate ions.

Brown crystals of **6** and red crystals of **7** suitable for a diffraction analysis were obtained by slow evaporation of these compounds in *n*-hexane–$CH_2Cl_2$ at room temperature. Perspective views of the molecular structures of complexes **6** and **7** are shown in Figs. 6 and 7, respectively, and relevant bond parameters in Tables 7 and 8, respectively. Cluster **7** was formulated initially as $[\{Os_5C(CO)_{14}(\mu\text{-}\eta^2\text{-}L')\}_2(\mu_4\text{-}Hg)]$ [L′ = SPh, SC(N=NPh)(=NNHPh)] based on spectroscopic evidence. This was further confirmed by single X-ray analysis. Notably, the cluster cores of **6** and **7** are the same. In each case, two pentanuclear $Os_5C$ units are linked by two edge-related osmium atoms to a central mercury atom. For each half of the molecule, the Hg atom asymmetrically bridges the 'hinge' bond of the bridged butterfly. The mercury bridges in the complexes are asymmetric, where Hg(1)–Os(1) and Hg(1)–Os(2) distances are 2.7703(8) and 3.0450(8) Å, in **6** (Fig. 6) and 2.7472(9) and 3.029(1) Å in **7** (Fig. 7), respectively. Along one open edge of this capped butterfly is a bridging SPh and SC(N=NPh)(=NNHPh) in **6** and **7** respectively, which are similar to that observed in the related clusters $[\{Ru_5C(CO)_{14}(\mu\text{-Cl})\}_2Hg_2Cl_2]$[15] and $[Ru_5C(CO)_{14}(\mu\text{-AuPPh}_3)(\mu\text{-Br})]$.[16] The presence of the mercury metal atom causes a lengthening of this Os–Os edge, hence the Os(1)–Os(2) bond lengths in **6** [2.946(1) Å] and **7** [2.912(1) Å] are the longest bonded Os–Os distances in the structure. The average bond length of the other Os–Os bonds is within the range normally recorded for the precursor, $[Os_5C(CO)_{15}]$[17] [2.88(2) and 2.85(3) Å]. The carbido-carbon remains at the centre of the 'bridged butterfly'. As in related carbide-centred clusters,[16,18] there are small differences in the Os–C(carbide) distance. The formation of **6** in this reaction is rather unusual because it involves the formation of a Ph–S moiety either before or after the assembly of the heterometallic cluster. Since we do

**Table 7** Selected bond lengths (Å) and angles (°) for complex **6**

| | | | |
|---|---|---|---|
| Hg(1)–Os(1) | 2.7703(8) | Hg(1)–Os(2) | 3.0450(8) |
| Os(1)–Os(2) | 2.946(1) | Os(1)–Os(3) | 2.849(1) |
| Os(1)–Os(5) | 2.849(1) | Os(2)–Os(3) | 2.883(1) |
| Os(2)–Os(5) | 2.880(1) | Os(3)–Os(4) | 2.925(1) |
| Os(4)–Os(5) | 2.922(1) | Os(1)–C(15) | 2.09(2) |
| Os(1)–S(1) | 2.463(5) | Os(4)–S(1) | 2.490(5) |
| S(1)–C(16) | 1.81(2) | | |
| | | | |
| Os(1)–Hg(1)–Os(2) | 60.65(2) | Hg(1)–Os(1)–Os(2) | 64.29(2) |
| Hg(1)–Os(2)–Os(1) | 55.06(2) | Os(2)–Os(1)–Os(3) | 59.65(3) |
| Os(2)–Os(1)–Os(5) | 59.57(3) | Os(3)–Os(1)–Os(5) | 89.43(3) |
| Os(1)–Os(2)–Os(3) | 58.50(3) | Os(1)–Os(2)–Os(5) | 58.55(3) |
| Os(3)–Os(2)–Os(5) | 88.15(3) | Os(1)–Os(3)–Os(4) | 75.21(3) |
| Os(2)–Os(3)–Os(4) | 89.05(3) | Os(1)–S(1)–Os(4) | 90.7(2) |

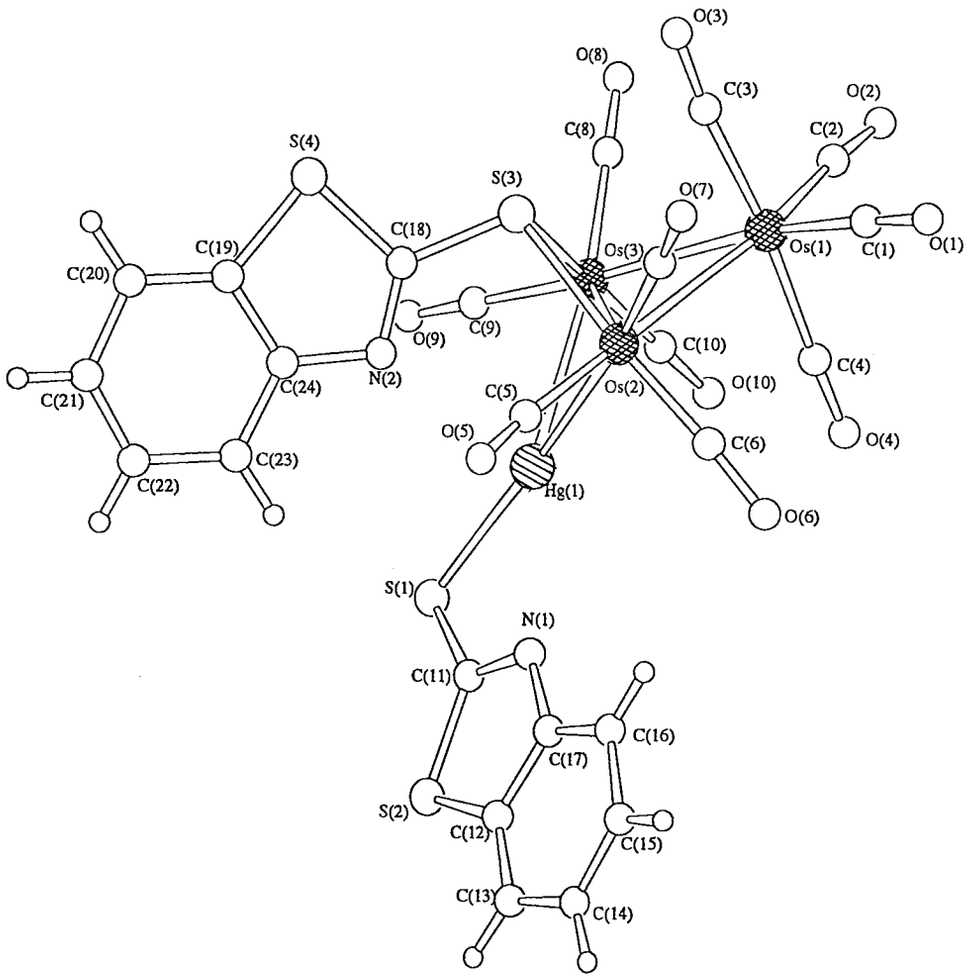


**Fig. 5** A perspective drawing of the molecular structure of **5**.

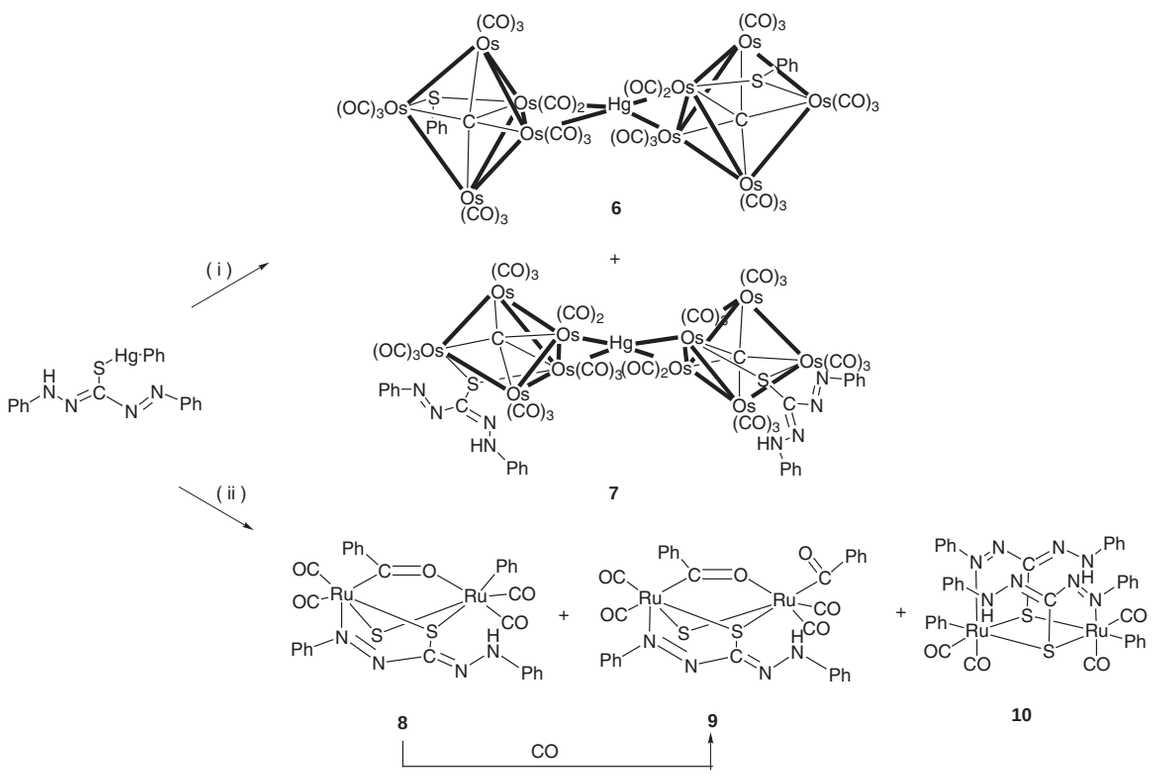


**Scheme 2** (i) $Os_5C(CO)_{15}$ in refluxing $CHCl_3$; (ii) $Ru_3(CO)_{12}$ in refluxing $CHCl_3$.

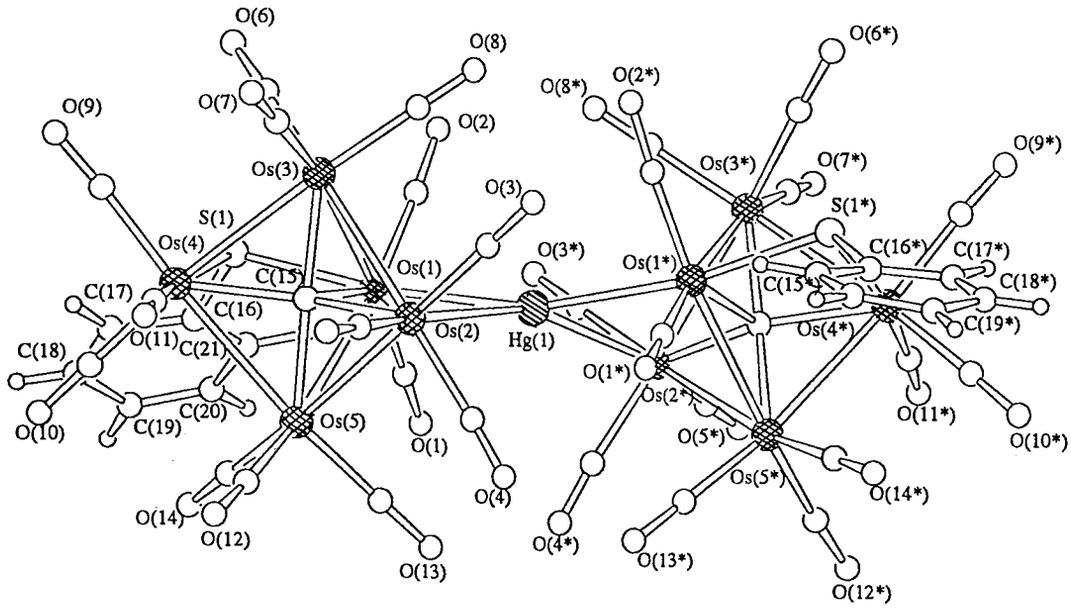


**Fig. 6** A perspective drawing of the molecular structure of **6**.

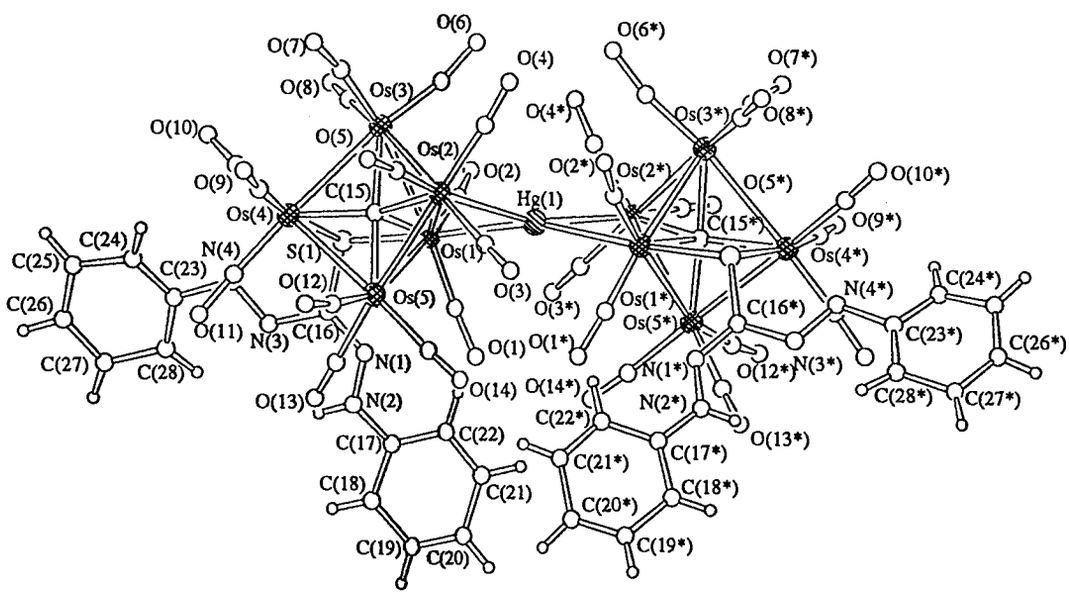


**Fig. 7** A perspective drawing of the molecular structure of **7**.

not observe the conversion of **1** to **6** under our experimental condition, it is tempting to suggest that the Ph–S fragment was formed earlier.

### Synthesis of $[Ru_2(CO)_4Ph\{\mu\text{-}\eta^2\text{-}C(O)Ph\}(\mu_2\text{-}S)(\mu\text{-}\eta^2\text{-}L')]$ 8, $[Ru_2(CO)_4\{C(O)Ph\}\{\mu\text{-}\eta^2\text{-}C(O)Ph\}(\mu_2\text{-}S)(\mu\text{-}\eta^2\text{-}L')]$ 9 and $[\{Ru(CO)_2Ph\}_2(\mu\text{-}\eta^2\text{-}L')_2]$ 10

The reaction of $[Ru_3(CO)_{12}]$ with [PhHg{SC(N=NPh)(=N-NHPh)}] in refluxing chloroform ($CHCl_3$) does not yield mixed-metal clusters, which is expected from the reactions involving organomercurials, but leads to the formation of three binuclear ruthenium carbonyl compounds $[Ru_2(CO)_4Ph\{\mu\text{-}\eta^2\text{-}C(O)Ph\}(\mu_2\text{-}S)(\mu\text{-}\eta^2\text{-}L')]$ **8**, $[Ru_2(CO)_4\{C(O)Ph\}\{\mu\text{-}\eta^2\text{-}C(O)Ph\}(\mu_2\text{-}S)(\mu\text{-}\eta^2\text{-}L')]$ **9** and $[\{Ru(CO)_2Ph\}_2(\mu\text{-}\eta^2\text{-}L')_2]$ **10** in 15, 15 and 45% yields, respectively (Scheme 2). In addition, $[Ru_3(CO)_{12}]$ and mercury metal were also obtained. Complexes **8**, **9** and **10** were isolated in pure form by preparative thin layer chromatography (TLC) on silica. Only terminal carbonyl activity was observed in the carbonyl absorption region of the solution IR spectra of **8**, **9** and **10** in dichloromethane (Table 1). Moreover, the IR spectra in KBr showed signals at 1563 $cm^{-1}$ (for **8**) and 1561 $cm^{-1}$ (for **9**) which are assigned to the coordinated acyl group. These values are comparable to those of other acyl complexes we reported earlier.[19] The proton NMR spectra recorded in dichloromethane-$d_2$ confirm the presence of the organic ligands and the absence of metal hydrides. The signals

**Table 8** Selected bond lengths (Å) and angles (°) for complex **7**

| | | | |
|---|---|---|---|
| Hg(1)–Os(1) | 2.7472(9) | Hg(1)–Os(2) | 3.029(1) |
| Os(1)–Os(2) | 2.912(1) | Os(1)–Os(3) | 2.857(2) |
| Os(1)–Os(5) | 2.865(2) | Os(2)–Os(3) | 2.869(2) |
| Os(2)–Os(5) | 2.877(2) | Os(3)–Os(4) | 2.928(2) |
| Os(4)–Os(5) | 2.923(2) | Os(1)–C(15) | 2.10(2) |
| Os(1)–S(1) | 2.436(5) | Os(4)–S(1) | 2.489(6) |
| N(1)–N(2) | 1.29(3) | N(3)–N(4) | 1.27(3) |
| N(2)–H(1) | 0.84 | S(1)–C(16) | 1.74(3) |
| | | | |
| Os(1)–Hg(1)–Os(2) | 60.32(3) | Hg(1)–Os(1)–Os(2) | 64.64(3) |
| Hg(1)–Os(2)–Os(1) | 55.04(3) | Os(2)–Os(1)–Os(3) | 59.63(4) |
| Os(2)–Os(1)–Os(5) | 59.72(4) | Os(3)–Os(1)–Os(5) | 88.49(4) |
| Os(1)–Os(2)–Os(3) | 59.22(4) | Os(1)–Os(2)–Os(5) | 59.33(4) |
| Os(3)–Os(2)–Os(5) | 88.03(4) | Os(1)–Os(3)–Os(4) | 74.57(4) |
| Os(2)–Os(3)–Os(4) | 90.45(5) | Os(1)–S(1)–Os(4) | 90.7(2) |

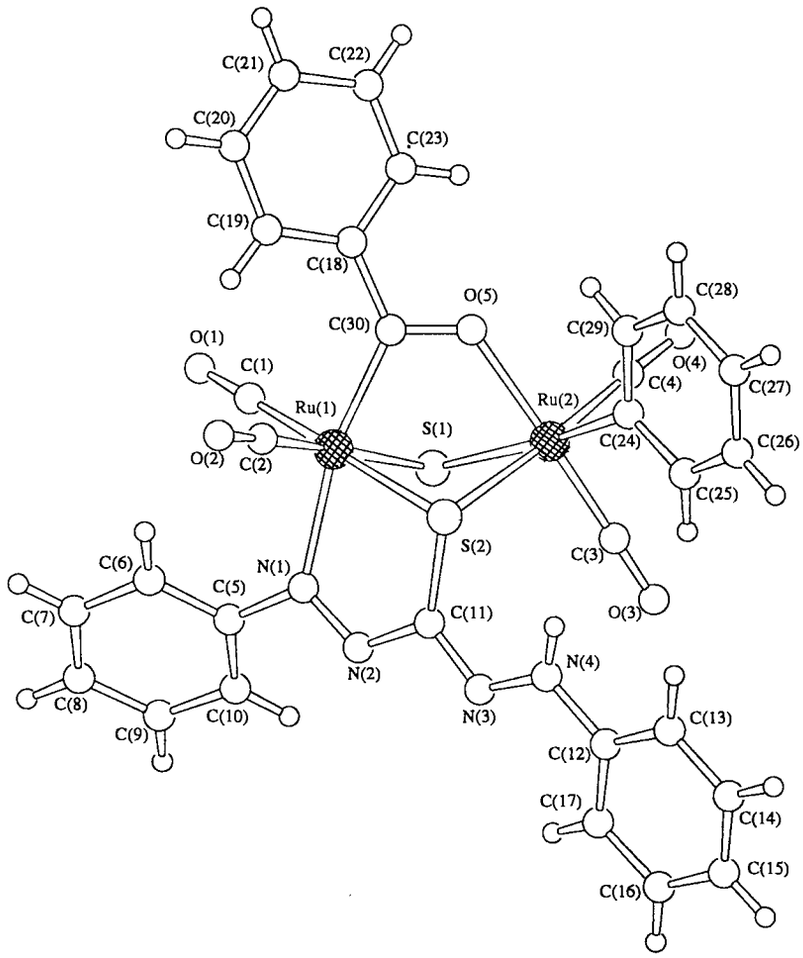


**Fig. 8** A perspective drawing of the molecular structure of **8**.

**Table 9** Selected bond lengths (Å) and angles (°) for complex **8**

| | | | |
|---|---|---|---|
| Ru(1)–S(1) | 2.4563(9) | Ru(2)–S(1) | 2.5406(9) |
| Ru(1)–S(2) | 2.4085(9) | Ru(2)–S(2) | 2.466(1) |
| Ru(1)–N(1) | 2.190(3) | Ru(1)–C(30) | 2.046(4) |
| Ru(2)–O(5) | 2.121(2) | Ru(1)–C(1) | 1.906(4) |
| Ru(1)–C(2) | 1.850(4) | Ru(2)–C(3) | 1.836(4) |
| Ru(2)–C(4) | 1.866(5) | Ru(2)–C(24) | 2.081(4) |
| S(2)–C(11) | 1.768(4) | N(1)–N(2) | 1.280(4) |
| N(3)–N(4) | 1.307(4) | C(30)–O(5) | 1.260(4) |
| C(18)–C(30) | 1.480(5) | N(4)–H(21) | 0.84 |
| Ru(1)···Ru(2) | 3.362(1) | S(1)···S(2) | 3.29(1) |
| | | | |
| Ru(1)–S(1)–Ru(2) | 84.43(3) | Ru(1)–S(2)–Ru(2) | 87.09(3) |
| S(1)–Ru(1)–S(2) | 85.11(3) | S(1)–Ru(2)–S(2) | 82.16(3) |
| S(1)–Ru(1)–C(2) | 176.8(1) | S(2)–Ru(1)–C(1) | 175.5(1) |
| S(1)–Ru(1)–N(1) | 84.58(8) | S(2)–Ru(1)–N(1) | 79.98(8) |
| S(1)–Ru(1)–C(30) | 86.15(10) | S(2)–Ru(1)–C(30) | 89.46(10) |
| S(1)–Ru(2)–C(3) | 95.0(1) | S(1)–Ru(2)–C(4) | 101.1(1) |
| S(1)–Ru(2)–C(24) | 170.35(10) | S(2)–Ru(2)–C(3) | 96.7(1) |
| S(2)–Ru(2)–C(4) | 173.7(1) | S(2)–Ru(2)–C(24) | 90.8(1) |
| S(1)–Ru(2)–O(5) | 82.24(6) | S(2)–Ru(2)–O(5) | 83.52(7) |
| Ru(1)–C(30)–O(5) | 116.1(2) | Ru(2)–O(5)–C(30) | 124.2(2) |

**Table 10** Selected bond lengths (Å) and angles (°) for complex **9**

| | | | |
|---|---|---|---|
| Ru(1)–S(1) | 2.396(2) | Ru(2)–S(1) | 2.458(2) |
| Ru(1)–S(2) | 2.461(2) | Ru(2)–S(2) | 2.578(2) |
| Ru(1)–N(1) | 2.190(6) | Ru(1)–C(31) | 2.036(7) |
| Ru(2)–O(7) | 2.116(4) | Ru(1)–C(1) | 1.851(8) |
| Ru(1)–C(2) | 1.897(8) | Ru(2)–C(3) | 1.866(8) |
| Ru(2)–C(4) | 1.894(7) | Ru(2)–C(5) | 2.052(8) |
| C(1)–O(1) | 1.150(10) | C(2)–O(2) | 1.133(10) |
| C(3)–O(3) | 1.126(10) | C(4)–O(4) | 1.135(9) |
| C(5)–O(5) | 1.226(9) | C(31)–O(7) | 1.276(7) |
| C(5)–C(25) | 1.53(1) | C(19)–C(31) | 1.472(10) |
| S(1)–C(12) | 1.766(8) | N(1)–N(2) | 1.280(7) |
| N(3)–N(4) | 1.324(9) | N(4)–H(21) | 1.11 |
| Ru(1)···Ru(2) | 3.382(1) | S(1)···S(2) | 3.30(1) |
| | | | |
| Ru(1)–S(1)–Ru(2) | 88.33(6) | Ru(1)–S(2)–Ru(2) | 84.29(6) |
| S(1)–Ru(1)–S(2) | 85.56(6) | S(1)–Ru(2)–S(2) | 81.80(6) |
| S(1)–Ru(1)–C(2) | 176.0(3) | S(2)–Ru(1)–C(1) | 176.7(2) |
| S(1)–Ru(1)–N(1) | 79.5(1) | S(2)–Ru(1)–N(1) | 85.0(1) |
| S(1)–Ru(1)–C(31) | 88.6(2) | S(2)–Ru(1)–C(31) | 85.8(2) |
| S(1)–Ru(2)–C(3) | 99.1(2) | S(1)–Ru(2)–C(4) | 171.6(2) |
| S(1)–Ru(2)–C(5) | 87.7(2) | S(2)–Ru(2)–C(3) | 94.2(2) |
| S(2)–Ru(2)–C(4) | 99.2(2) | S(2)–Ru(2)–C(5) | 169.3(2) |
| S(1)–Ru(2)–O(7) | 81.7(1) | S(2)–Ru(2)–O(7) | 82.2(1) |
| Ru(1)–C(31)–O(7) | 116.4(5) | Ru(2)–O(7)–C(31) | 124.1(4) |

at $\delta$ 9.15, 11.75 and 8.90 in complexes **8**, **9** and **10**, respectively, are assigned to the NH protons of the dithizonate ion. The FAB mass spectra of **8**, **9** and **10** show parent ion peaks at $m/z$ = 788, 811 and 980, with each showing subsequent and sequential loss of four carbonyl ligands.

Red crystals of **8**, **9** and **10** suitable for X-ray analysis were obtained from $CH_2Cl_2$–cyclohexane or *n*-hexane–$CH_2Cl_2$ solutions at room temperature. Perspective drawings of complexes **8**, **9** and **10** are shown in Figs. 8, 9 and 10 respectively, with selected bond lengths and angles given in Tables 9, 10, and 11 respectively. One molecule of water and cyclohexane, as the solvent of crystallization, was present in the asymmetric units of **9** and **10**, respectively. As in Figs. 8 and 9, the Ru atoms are bridged diaxially by an acyl group, [μ-η$^2$-C(O)Ph], and bridged diequatorially by a sulfido group, [SC(N=NPh)(=NNHPh)]. The lone pair of the oxygen atom bond to Ru(2) forming a μ-η$^2$

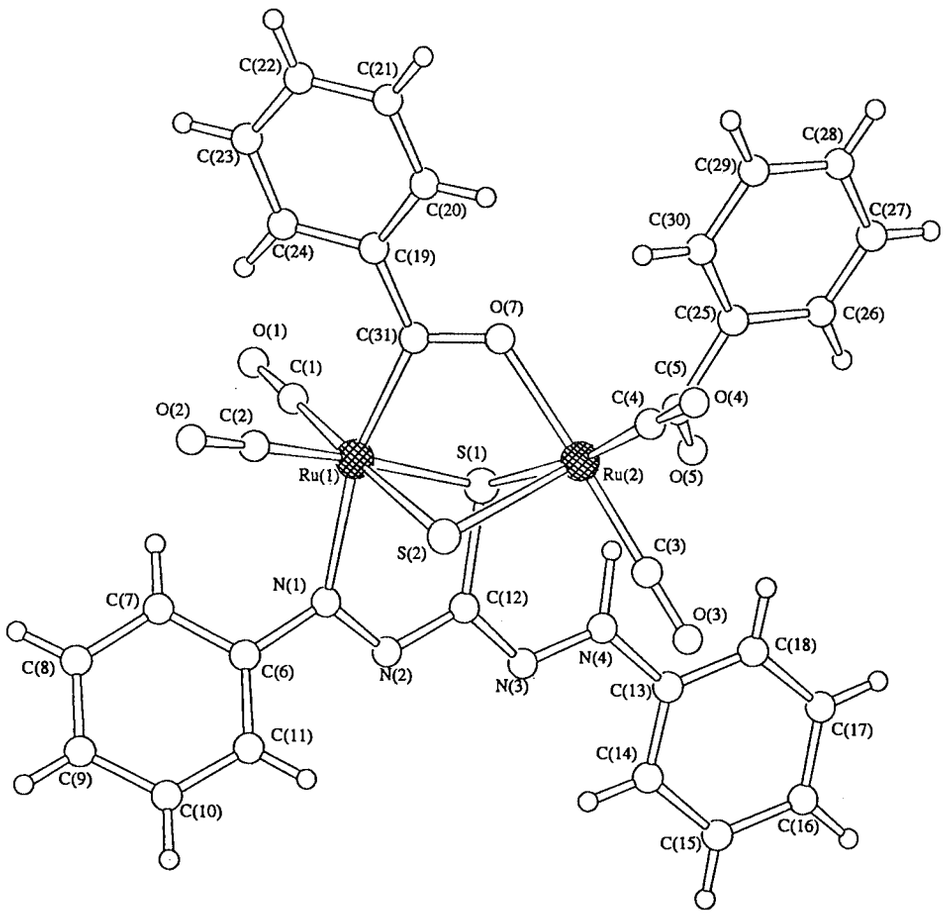


**Fig. 9** A perspective drawing of the molecular structure of **9**.

**Table 11** Selected bond lengths (Å) and angles (°) for complex **10**

| | | | |
|---|---|---|---|
| Ru(1)–S(1) | 2.431(1) | Ru(2)–S(1) | 2.485(1) |
| Ru(1)–S(2) | 2.572(1) | Ru(2)–S(2) | 2.427(1) |
| Ru(1)–N(1) | 2.137(4) | Ru(2)–N(8) | 2.203(4) |
| Ru(1)–C(1) | 1.888(5) | Ru(1)–C(2) | 1.872(5) |
| Ru(1)–C(18) | 2.118(5) | Ru(2)–C(3) | 1.87(5) |
| Ru(2)–C(4) | 1.874(6) | Ru(2)–C(24) | 2.112(5) |
| S(1)–C(11) | 1.78(5) | S(2)–C(36) | 1.773(5) |
| N(1)–N(2) | 1.281(5) | N(3)–N(4) | 1.322(5) |
| N(5)–N(6) | 1.311(5) | N(7)–N(8) | 1.286(5) |
| N(1)–C(5) | 1.440(6) | N(4)–C(12) | 1.406(6) |
| N(5)–C(30) | 1.414(6) | N(8)–C(37) | 1.434(5) |
| N(4)–H(46) | 0.84 | N(5)–H(45) | 0.84 |
| Ru(1)···Ru(2) | 3.713(1) | S(1)···S(2) | 3.25(1) |
| | | | |
| Ru(1)–S(1)–Ru(2) | 97.95(4) | Ru(1)–S(2)–Ru(2) | 95.73(4) |
| S(1)–Ru(1)–S(2) | 80.86(4) | S(1)–Ru(2)–S(2) | 82.73(4) |
| S(1)–Ru(1)–C(1) | 95.5(1) | S(1)–Ru(1)–C(2) | 178.4(1) |
| S(1)–Ru(2)–C(3) | 91.5(2) | S(1)–Ru(2)–C(24) | 86.5(1) |
| S(2)–Ru(1)–C(1) | 90.8(2) | S(2)–Ru(1)–C(18) | 171.9(1) |
| S(2)–Ru(2)–C(4) | 95.0(2) | S(2)–Ru(2)–C(24) | 91.5(1) |

acyl bridge along the Ru···Ru line. A phenyl group is coordinated to Ru(2) which resulted from the cleavage of an Hg–C bond in the organomercurial. The plane of the aryldiazo ligand was parallel to the Ru···Ru line, which occupies an $\eta^2$-bridging site with Ru(1)–C(30) [2.046(4) Å] and Ru(2)–O(5) [2.121(2) Å] in **8** and Ru(1)–C(31) [2.036(7) Å] and Ru(2)–O(7) [2.116(4) Å] in **9**. The $Ru_2S_2$ core is not planar, but bent in a butterfly fashion which results in a fold angle of 131.87° in **8** and **9**. This bending results in a mean Ru–Ru separation of 3.37 Å in both complexes, which is comparable to the non-bonding distance observed in $[(\eta^6\text{-}C_6H_6)Ru(\mu\text{-}OMe)_3Ru(\eta^6\text{-}C_6H_6)][BPh_4]$[20] [3.005(2) Å]. Subsequent reductive elimination of benzene is usually favoured, as soon as a hydride ligand is available. However, in the absence of such a hydride ligand in **9**, a migratory CO insertion takes place to yield the terminal acyl group, [C(O)Ph]. The PhCO ligand is formed by Hg–Ph bond cleavage and Ph migration to CO. Similar observations are also found in $[Os_3(\mu\text{-}Ph)(\mu\text{-}PhCO)(\mu_3\text{-}Se)_2(CO)_8]$[21] and $[Ru_3\{\mu\text{-}\eta^2\text{-}C(O)Ph\}\{\mu_3\text{-}\eta^2\text{-}P(Ph)(C_5H_4N)\}(CO)_9]$.[22] The sulfido, [SC(N=NPh)(=NNHPh)] and [$\mu$-$\eta^2$-C(O)Ph] moieties act as four-, five- and three-electron donors, respectively, which result in a total 36 CVE in both complexes and are in agreement with the Condensed Polyhedra Method for binuclear complexes with no metal–metal bonds.[23]

As mentioned before, the molecular structures of **8** and **9** are different in a CO insertion at Ru(2)–Ph. It is of interest to know whether the addition of CO would lead to the formation of complex **9** from **8**. Thus, a stream of CO gas was bubbled through a solution of **8** at room temperature. IR and spot TLC monitoring indicated the quantitative formation of **9**, accompanied with unreacted starting material. Therefore **8** appears to be an intermediate in the formation of **9** by Ru-assisted insertion of a CO molecule into the Ru–Ph moiety. By contrast, heating of complex **9** in refluxing *n*-hexane for 4 h resulted in no visible change as indicated by IR and spot TLC monitoring. Therefore, complex **9** is thermally stable up to the refluxing temperature of *n*-hexane without molecular rearrangements or decomposition.

X-Ray analysis of **10** revealed that the structure consists of two $Ru(CO)_2$ fragments which are held together by two [$\mu$-$\eta^2$-$SC(N{=}NPh)(=NNHPh)_2$] moieties, bonded through a sulfur and nitrogen [N(1)–Ru(1) 2.137(4) Å and N(8)–Ru(2) 2.203(4) Å] in *syn* arrangements with respect to the $Ru_2S_2$ plane. The central Ru(1)–S(1)–Ru(2)–S(2) is not planar, but adopts an envelope conformation which is folded at an angle of 163.48° with respect to the S(1)···S(2) line. The ligands are essentially planar and *syn*-coordinated to the ruthenium–sulfur rhombus

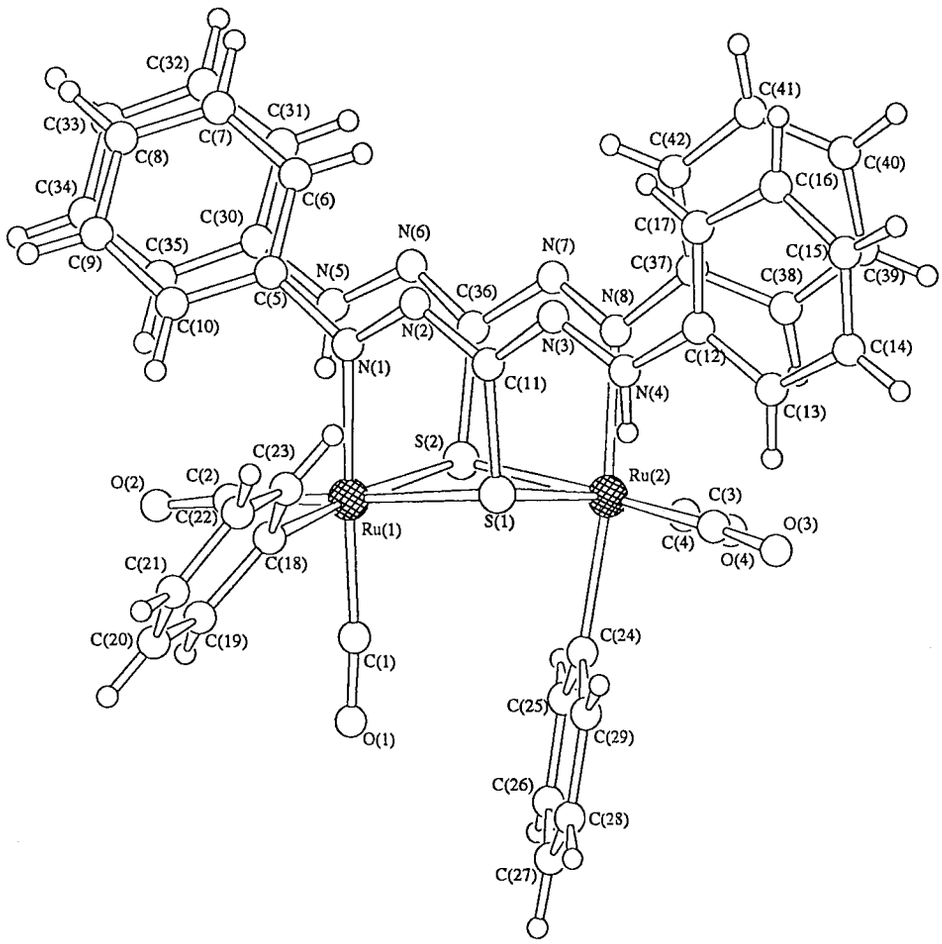


**Fig. 10** A perspective drawing of the molecular structure of **10**.

array (dihedral angles 96.8 and 79.29°). The intermetallic distance of **10** (3.71 Å) is too long to indicate any significant interactions between the two ruthenium atoms (*cf.* average Ru–Ru 2.85(4) Å in $[Ru_3(CO)_{12}]$[24]). A phenyl group was unexpectedly coordinated which the ruthenium atoms that originated from the cleavage of an Hg–C bond in [PhHgSC(N=NPh)(=NNHPh)], as in complex **8**. The Ru–C(Ph) bond in both complexes has a mean distance of 2.11(5) Å, which is similar to that in $[(C_5Me_5)Ru(NO)(C_6H_5)(O_3SCF_3)]$[25] [2.10(5) Å].

Recently, we have reported that the reaction of the mercurial complex, [PhHg{SC(N=NPh)(=NNHPh)}] with an activated triosmium carbonyl cluster $[Os_3(CO)_{10}(NCMe)_2]$, formed a pair of binuclear osmium carbonyl isomers $[\{Os(CO)_2Ph\}_2(\mu\text{-}\eta^2\text{-}L')_2]$[26] which was isostructural with **10**. However, no analogous complexes of **8** and **9** were observed in this reaction. Presumably this is due to a higher kinetic stability of Os complexes, which makes CO insertion more difficult.

## Conclusion

We have observed previously that the reaction of $[Os_3(CO)_{10}(\mu\text{-}H)_2]$ with organomercury compounds possessing a nucleophilic –C≡C– functionality yields a series of osmium–mercury cluster complexes having the following structures: (1) two Os–Hg mixed-metal butterflies sharing a central wingtip mercury atom, and (2) a central $Os(CO)_4$ fragment with two *cis*-coordinated metal butterflies.[6b] Clusters **1**–**4**, **6** and **7** are analogous complexes which demonstrated that the Hg atom could act as a 'linker'. Cluster **5** contains ligand and Hg–ligand moieties that share the same edge of the Os–Os bond. The reaction of $[Os_5C(CO)_{15}]$ with [PhHgSC(N=NPh)(=NNHPh)] resulted in clusters **6** and **7** where two $\{Os_5C(CO)_{14}\}$ moieties were linked by a mercury atom. However, in the case of ruthenium carbonyl complexes, this reaction resulted in binuclear ruthenium carbonyl complexes **8**–**10** with no metal–metal bonds instead of the usual mixed-metal clusters.

## Experimental

All reactions and manipulations were carried out under an inert atmosphere using standard Schlenk techniques. Solvents were freshly purified by standard procedures prior to use. All chemicals, except where stated, were obtained commercially and used as received. The complexes $[PhHgS(C_5H_4N)]$[27] and [PhHg(mbt)][28] were prepared by literature methods. IR spectra were recorded on a Bio-Rad FTS-7 IR spectrometer, using 0.5 mm calcium fluoride solution cells. The proton NMR spectra were recorded on a Bruker DPX 300 NMR spectrometer using $CD_2Cl_2$ and referenced to $SiMe_4$ ($\delta$ 0). Mass spectra were recorded on a Finnigan MAT 95 instrument by fast atom bombardment techniques, using *m*-nitrobenzyl alcohol as the matrix solvent. Routine purification of products was carried out in air by thin layer chromatography (TLC) on plates coated with Merck Kieselgel 60 $GF_{254}$.

### Reaction of $[Os_3(CO)_{10}(NCMe)_2]$ with $[PhHgS(C_5H_4N)]$

A yellow solution of $[Os_3(CO)_{10}(NCMe)_2]$ (500 mg, 0.536 mmol) in $CH_2Cl_2$ was stirred with 1 equivalent of $[PhHgS(C_5H_4N)]$ (208 mg, 0.54 mmol) under $N_2$. The colour gradually turned red and powdery mercury was also deposited. Stirring was continued until all starting materials were consumed (TLC monitoring, *ca.* 2 h). The reaction mixture was then

filtered to remove the very fine powder of mercury and the filtrate was evaporated *in vacuo*. The residue was finally redissolved in $CH_2Cl_2$ (*ca.* 2 $cm^3$) and separated by preparative TLC using *n*-hexane–$CH_2Cl_2$ (7:3 v/v) as the eluent to afford two bands with $R_f$ *ca.* 0.7 and 0.55, which were extracted from silica to yield yellow complex **1** (352 mg, 0.134 mmol, 25%) and orange complex **2** (341 mg, 0.161 mmol, 30%) respectively (Found: C, 15.41; H, 0.30; N, 1.09. Calc. for $C_{34}H_8Hg_2N_2O_{24}Os_7S_2$ **1**: C, 15.42; H, 0.30; N, 1.07%. Found: C, 16.98; H, 0.37; N, 1.30. Calc. for $C_{30}H_8HgN_2O_{20}Os_6S_2$ **2**: C, 16.96; H, 0.38; N, 1.32%).

### Reaction of $[Ru_3(CO)_{10}(NCMe)_2]$ with $[PhHgS(C_5H_4N)]$

To a $CH_2Cl_2$ solution of freshly prepared $[Ru_3(CO)_{10}(NCMe)_2]$ (85 mg, 0.128 mmol), $[PhHgS(C_5H_4N)]$ (49 mg, 0.128 mmol) was added at room temperature. The reaction mixture gradually changed from pale yellow to red upon addition. Reactions were completed after stirring for 1 h, as monitored by TLC and IR. The reaction solution was concentrated *in vacuo* and the residue redissolved in $CH_2Cl_2$ (*ca.* 2 $cm^3$) and separated by TLC using *n*-hexane–$CH_2Cl_2$ (1:1 v/v). This afforded $[Ru_3(CO)_{12}]$ and a red complex **3** (119.51 mg, 0.061 mmol, 48%) with $R_f$ *ca.* 0.5 as the sole product (Found: C, 19.69; H, 0.42; N, 1.47. Calc. for $C_{32}H_8Hg_2N_2O_{22}Ru_7S_2$ **2**: C, 19.74; H, 0.41; N, 1.44%).

### Reaction of $[Os_3(CO)_{10}(NCMe)_2]$ with [PhHgS(mbt)] (Hmbt = 2-mercaptobenzothiazole)

A yellow solution of $[Os_3(CO)_{10}(NCMe)_2]$ (500 mg, 0.536 mmol) in $CH_2Cl_2$ was stirred with 1 equivalent of [PhHg(mbt)] (239 mg, 0.54 mmol) under $N_2$. The colour gradually turned orange–red and powdery mercury was deposited. Stirring was continued until all starting materials were consumed (TLC monitoring, *ca.* 1.5 h). The reaction mixture was then filtered to remove the very fine powder of mercury and the filtrate was evaporated *in vacuo*. The residue was finally redissolved in $CH_2Cl_2$ (*ca.* 2 $cm^3$) and separated by preparative TLC using *n*-hexane–$CH_2Cl_2$ (3:2 v/v) as the eluent to afford two bands with $R_f$ *ca.* 0.8 and 0.65, which were extracted from silica to yield orange complex **4** (419 mg, 0.188 mmol, 35%) and yellow complex **5** (149 mg, 0.107 mmol, 20%), respectively (Found: C, 18.29; H, 0.40; N, 1.25. Calc. for $C_{34}H_8HgN_2O_{20}Os_6S_4$ **4**: C, 18.26; H, 0.36; N, 1.25. Found: C, 20.75; H, 0.89; N, 2.04. Calc. for $C_{24}H_{12}HgN_2O_{10}Os_3S_4$ **5**: C, 20.75; H, 0.86; N, 2.02%).

### Thermolysis of cluster 5

Cluster **5** (100 mg, 0.072 mmol) was refluxed in $CHCl_3$ under an inert atmosphere. The reaction was monitored by TLC and IR and completed after about 6 h. The solvent was then removed *in vacuo* and redissolved in $CH_2Cl_2$ (3 $cm^3$). TLC purification (eluent: *n*-hexane–$CH_2Cl_2$ (1:1 v/v)) afforded **4** (58 mg, 0.026 mmol, 36%) and unreacted starting material **5** (5 mg, 0.004 mmol, 5%).

### Reaction of $[Os_5C(CO)_{15}]$ with [PhHgSC(N=NPh)(=NNHPh)]

$[Os_5C(CO)_{15}]$ (500 mg, 0.361 mmol) and [PhHgSC(N=NPh)(=NNHPh)] (191 mg, 0.361 mmol) were stirred at reflux in $CHCl_3$ (150 ml) for 12 h after all starting materials had been consumed. The colour gradually turned from yellow to reddish brown. After reduction in volume, the filtrate was separated by preparative TLC on silica with an eluent of *n*-hexane–$CH_2Cl_2$ (3:2 v/v) to give two bands which were extracted from silica to yield red complex **6** ($R_f$ *ca.* 0.85, 294 mg, 0.094 mmol, 26%) and purple complex **7** ($R_f$ *ca.* 0.55, 420 mg, 0.123 mmol, 34%) (Found: C, 16.14; H, 0.33. Calc. for $C_{42}H_{10}HgO_{28}Os_{10}S_2$ **6**: C, 16.11; H, 0.32. Found: C, 19.67; H, 0.60; N, 3.28. Calc. for $C_{56}H_{20}HgN_8O_{28}Os_{10}S_2$ **7**: C, 19.65; H, 0.58; N, 3.28%).

### Reaction of $[Ru_3(CO)_{12}]$ with [PhHgSC(N=NPh)(=NNHPh)]

$[Ru_3(CO)_{12}]$ (639 mg, 1.0 mmol) and [PhHgSC(N=NPh)(=NNHPh)] (530 mg, 1.0 mmol) were dissolved in 50 $cm^3$ of $CHCl_3$ and the dark red solution allowed to reflux for 3 h. The reaction mixture was then filtered to remove the very fine powder of mercury and excess solvent was removed under reduced pressure, yielding a deep brown residue. This residue was then dissolved in a minimum amount of $CH_2Cl_2$ and subject to preparative TLC on silica using *n*-hexane–$CH_2Cl_2$ (1:1 v/v) as eluent. Other than the traces of $[Ru_3(CO)_{12}]$, two orange and one red bands with $R_f$ *ca.* 0.85, 0.7 and 0.5, respectively were obtained and characterized as **8** (118 mg, 0.15 mmol, 15%), **9** (122 mg, 0.15 mmol, 15%) and **10** (442 mg, 0.456 mmol, 45%), respectively (Found: C, 46.01; H, 2.69; N, 7.17. Calc. for $C_{30}H_{21}N_4O_5Ru_2S_2$ **8**: C, 45.98; H, 2.68; N, 7.15. Found: C, 45.80; H, 2.60; N, 6.90. Calc. for $C_{31}H_{23}N_4O_7Ru_2S_2$ **9**: C, 45.82; H, 2.59; N, 6.90. Found: C, 51.38; H, 3.45; N, 11.43. Calc. for $C_{42}H_{34}N_8O_4Ru_2S_2$ **10**: C, 51.37; H, 3.47; N, 11.41%).

### Carbonylation of complex 8 in $CH_2Cl_2$

Complex **8** (20 mg, 0.025 mmol) was dissolved in $CH_2Cl_2$ (30 ml) and the orange solution stirred at room temperature for 6 h. The solvent was removed under reduced pressure and the only product isolated by TLC, using *n*-hexane–$CH_2Cl_2$ (1:1, v/v) as the eluent, was **9** ($R_f$ = 0.85, 15 mg, 0.02 mmol, 75%) accompanied by a small amount of unreacted **8** ($R_f$ = 0.7, 3 mg, 0.003 mmol, 15%).

### Thermolysis of complex 9

Complex **9** (20 mg, 0.025 mmol) was dissolved in *n*-hexane (30 ml). The orange solution was refluxed under a dinitrogen atmosphere. Using IR spectroscopic monitoring, no visible change was observed after 4 h.

### Crystallography

All pertinent crystallographic data and other experimental details are summarized in Table 12. Intensity data were collected at ambient temperature on either a Rigaku AFC7R diffractometer (complexes **1**, **2** and **3**) or a MAR research image plate scanner (complexes **4**–**10**) equipped with graphite-crystal monochromated Mo-Kα radiation ($\lambda$ = 0.71073 Å) using $\omega$–$2\theta$ and $\omega$ scan types, respectively. The diffracted intensities were corrected for Lorentz and polarization effects. Absorption correction by $\varphi$-scan techniques was done for **1**, **2** and **3**. However, for complexes **4**–**10**, an approximate absorption correction by interimage scaling was also applied. Scattering factors were taken from ref. 29(*a*) and anomalous dispersion effects[29b] were included in $F_c$. The structures were solved by direct methods (SIR88[30] for **10**; SIR92[31] for **4**, **5**; SHELX86[32] for **1**–**3** and **6**–**9**) and expanded by Fourier-difference techniques (DIRDIF94).[33] The solutions were refined by full-matrix least-squares analysis on *F*. For all structures, the heavy atoms Hg, Os and S were refined anisotropically. Attempts to refine all the atoms anisotropically were made, however, in structures **1**–**4** and **7**, but led negative anisotropic displacement parameters. Therefore some non-hydrogen atoms were refined isotropically. Hydrogen atoms were generated in their ideal positions, except N(H) which were located from a difference Fourier synthesis and included in the structure factor calculations but not refined. Calculations were performed on a Silicon-Graphics computer, using the program package TEXSAN.[34]

CCDC reference number 186/1521.

See http://www.rsc.org/suppdata/dt/1999/2497/ for crystallographic files in .cif format.

**Table 12** Summary of crystal data and data collection parameters for compounds **1**–**10**

| | **1** | **2** | **3** | **4** | **5** | **6** | **7**·0.5$CH_2Cl_2$ | **8** | **9**·$H_2O$ | **10**·$C_6H_{12}$ |
|---|---|---|---|---|---|---|---|---|---|---|
| Empirical formula | $C_{34}H_8Hg_2N_2O_{24}Os_7S_2$ | $C_{30}H_8HgN_2O_{20}Os_6S_2$ | $C_{32}H_8Hg_2N_2O_{22}Ru_7S_2$ | $C_{34}H_8HgN_2O_{20}Os_6S_4$ | $C_{24}H_8HgN_2O_{10}Os_3S_4$ | $C_{42}H_{10}HgO_{28}Os_{10}S_2$ | $C_{57}Cl_2H_{22}HgN_8O_{28}Os_{10}S_2$ | $C_{30}H_{21}N_4O_5Ru_2S_2$ | $C_{31}H_{23}N_4O_7Ru_2S_2$ | $C_{48}H_{46}N_8O_4Ru_2S_2$ |
| $M$ | 2625.14 | 2122.30 | 1945.21 | 2234.47 | 1383.76 | 3129.23 | 3504.45 | 783.78 | 829.81 | 1065.20 |
| Crystal system | Triclinic | Monoclinic | Orthorhombic | Monoclinic | Monoclinic | Orthorhombic | Orthorhombic | Monoclinic | Monoclinic | Triclinic |
| Space group | $P\bar{1}$ (no. 2) | $P2_1/n$ (no. 14) | *Pbca* (no. 61) | $P2_1/n$ (no. 14) | $C2/c$ (no. 15) | *Pbcn* (no. 60) | *Pbcn* (no. 60) | $C2/c$ (no. 15) | $C2/c$ (no. 15) | $P\bar{1}$ (no. 2) |
| $a$/Å | 12.662(1) | 11.465(4) | 18.062(5) | 27.790(1) | 45.922(1) | 30.751(1) | 25.209(1) | 22.904(1) | 22.924(1) | 11.601(1) |
| $b$/Å | 14.943(1) | 24.612(5) | 32.879(5) | 9.216(1) | 9.233(1) | 13.957(1) | 17.109(1) | 10.221(1) | 10.417(1) | 12.608(1) |
| $c$/Å | 15.317(1) | 18.167(4) | 16.155(6) | 36.730(1) | 14.858(1) | 13.227(1) | 18.252(1) | 26.948(1) | 28.349(1) | 17.852(1) |
| $\alpha$/° | 106.66(1) | — | — | — | — | — | — | — | — | 80.26(1) |
| $\beta$/° | 107.62(1) | 107.81(2) | — | 100.53(1) | 93.88(1) | — | — | 103.65(1) | 100.01(1) | 73.73(1) |
| $\gamma$/° | 99.47(1) | — | — | — | — | — | — | — | — | 71.21(1) |
| $U$/Å$^3$ | 2543.9(5) | 4880(2) | 9594(4) | 9248.6(9) | 6285.3(7) | 5676.9(5) | 7872.1(6) | 6130.4(7) | 6666.7(7) | 2364.1(4) |
| $Z$ | 2 | 4 | 8 | 8 | 8 | 4 | 4 | 8 | 8 | 2 |
| $\mu$(Mo-K$\alpha$)/cm$^{-1}$ | 235.82 | 188.41 | 86.96 | 199.81 | 172.87 | 251.24 | 182.04 | 11.67 | 10.83 | 7.79 |
| $T$/K | 298 | 298 | 298 | 298 | 298 | 298 | 298 | 298 | 298 | 298 |
| No. reflections collected | 21690 | 6955 | 6927 | 39915 | 24814 | 37971 | 29145 | 23216 | 22671 | 14273 |
| No. unique reflections | 7991 | 6574 | 6793 | 12406 | 5916 | 5591 | 6692 | 5775 | 5899 | 7994 |
| No. observed reflections [$I > 1.5\sigma(I)$] | 5048 | 3948 | 3089 | 5790 | 4250 | 3718 | 3537 | 4110 | 4358 | 5896 |
| $R^a$ | 0.082 | 0.089 | 0.067 | 0.085 | 0.062 | 0.054 | 0.059 | 0.035 | 0.053 | 0.042 |
| $R'^b$ | 0.090 | 0.084 | 0.055 | 0.084 | 0.070 | 0.053 | 0.048 | 0.035 | 0.061 | 0.050 |

$^a$ $R = \Sigma\big||F_o| - |F_c|\big| / |F_c|$. $^b$ $R' = [\Sigma w(|F_o| - |F_c|)^2/\Sigma w F_o^2]^{\frac{1}{2}}$.

## Acknowledgements

We gratefully acknowledge financial support from the Hong Kong Research Grants Council and the University of Hong Kong. F.-S. K. acknowledges the receipt of a post-graduate studentship administered by the University of Hong Kong.

## References

1 M. Ferrer, A. Perales, O. Rossel and M. Seco, *J. Chem. Soc.*, *Chem. Commun.*, 1990, 1447.
2 L. N. Zakharov, Y. T. Struchkov, S. N. Titova, V. T. Bychkov, G. A. Domrachev and G. A. Razumaez, *Cryst. Struct. Commun.*, 1980, **9**, 549.
3 A. Bianchini and L. J. Farrugia, *Organometallics*, 1992, **11**, 540.
4 E. Rosenberg, D. Ryckman, I. N. Hsu and R. W. Gellert, *Inorg. Chem.*, 1986, **25**, 194.
5 L. H. Gade, *Angew. Chem.*, *Int. Ed. Engl.*, 1993, **32**, 24.
6 (*a*) Y. K. Au and W. T. Wong, *J. Chem. Soc.*, *Dalton Trans.*, 1995, 1389; (*b*) Y. K. Au and W. T. Wong, *J. Chem. Soc.*, *Dalton Trans.*, 1996, 899; (*c*) Y. K. Au and W. T. Wong, *Inorg. Chem.*, 1997, **36**, 2092.
7 J. W. S. Hui and W. T. Wong, *J. Chem. Soc.*, *Dalton Trans.*, 1997, 2445; J. W. S. Hui and W. T. Wong, *J. Chem. Soc.*, *Dalton Trans.*, 1998, 2065.
8 C. Cathey, J. Lewis, P. R. Raithby and M. C. Ramirez de Arellano, *J. Chem. Soc.*, *Dalton Trans.*, 1994, 3331.
9 A. Bianchini and L. J. Farrugia, *Organometallics*, 1992, **11**, 540.
10 S. Hajela, B. M. Novak and E. Rosenberg, *Organometallics*, 1989, **8**, 468.
11 M. R. Churchill and B. G. Deboer, *Inorg. Chem.*, 1977, **16**, 878.
12 A. J. Deeming, K. I. Hardcastle and M. Karim, *Inorg. Chem.*, 1992, **31**, 4792.
13 M. R. Churchill and R. A. Lachewycz, *Inorg. Chem.*, 1979, **18**, 3261.
14 P. L. Andreu, J. A. Cabeza, A. Llamazares and V. Riera, *J. Organomet. Chem.*, 1991, **420**, 431.
15 B. F. G. Johnson, W. L. Kwik, J. Lewis, P. R. Raithby and V. P. Saharan, *J. Chem. Soc.*, *Dalton Trans.*, 1991, 1037.
16 B. F. G. Johnson, J. Lewis, S. W. Sankey, K. Wong, M. McPartlin and W. J. H. Nelson, *J. Organomet. Chem.*, 1980, **191**, C3.
17 P. F. Jackson, B. F. G. Johnson, J. Lewis and J. N. Nicholls, *J. Chem. Soc.*, *Chem. Commun.*, 1980, 564.
18 J. S. Bradley, R. L. Pruett, E. Hill, G. B. Ansell, M. E. Leonowicz and M. A. Modrick, *Organometallics*, 1982, **1**, 748.
19 S. M. Lee and W. T. Wong, *J. Cluster Sci.*, 1996, **7**, 37.
20 R. O. Gould, T. A. Stephenson and D. A. Tocher, *J. Organomet. Chem.*, 1984, **263**, 375.
21 A. J. Arce, P. Arrojo, A. J. Deeming and Y. de Sanctis, *J. Chem. Soc.*, *Chem. Commun.*, 1991, 1491.
22 N. Lugan, G. Lavigne and J. J. Bonnet, *Inorg. Chem.*, 1986, **25**, 9.
23 D. M. P. Mingos, *J. Chem. Soc.*, *Chem. Commun.*, 1982, 706.
24 M. R. Churchill, F. J. Hollander and J. P. Hutchison, *Inorg. Chem.*, 1977, **16**, 2655.
25 M. R. Burns and J. L. Hubbard, *J. Am. Chem. Soc.*, 1994, **116**, 9514.
26 F. S. Kong and W. T. Wong, unpublished results.
27 A. Castineiras, W. Hiller, J. Strahle, J. Bravo, J. S. Casas, M. Gayoso and J. Sordo, *J. Chem. Soc.*, *Dalton Trans.*, 1986, 1945.
28 J. Bravo, J. S. Casas, M. Castano, M. Gayoso, Y. P. Mascarenhas, A. Sanchez, C. de. O. P. Santos and J. Sordo, *Inorg. Chem.*, 1985, **24**, 3435.
29 D. T. Cromer and J. T. Waber, *International Tables for X-Ray Crystallography*, Kynoch Press, Birmingham, 1974, vol. 4, (*a*) Table 22B; (*b*) Table 2.3.1.
30 M. C. Burla, M. Camalli, G. Cascarano, C. Giacovazzo, G. Polidori, R. Spagna and D. Viterbo, *J. Appl. Crystallogr.*, 1989, **22**, 389.
31 A. Altomare, M. C. Burla, M. Camalli, M. Cascarano, G. Giacovazzo, A. Guagliardi and G. Polidori, SIR 92, *J. Appl. Crystallogr.*, 1994, **27**, 435.
32 G. M. Sheldrick, SHELXS 86, Program for Crystal Structure Solution, *Acta Crystallogr.*, *Sect. A*, 1990, **46**, 467.
33 DIRDIF94: B. T. Beurskens, G. Admiroal, G. Beurskens, W. P. Bosman, R. de Gelder, R. Isrel and J. M. M. Smits, Technical Report of the Crystallography Laboratory, University of Nijmegen, 1994.
34 TEXSAN, Crystal Structure Analysis Package, Molecular Structure Corporation, 1985 and 1992.

*Paper 9/02701G*